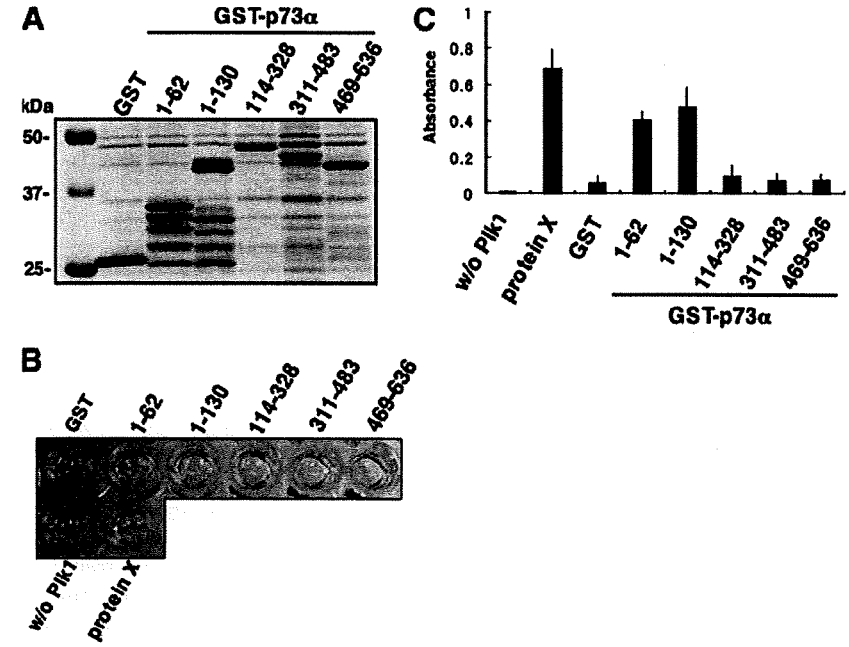

FIGURE 10. **Plk1 has an ability to phosphorylate p73 at its NH_2-terminal region *in vitro*.** *A*, Coomassie Brilliant Blue staining of GST or GST-p73α fusion proteins used for *in vitro* kinase reaction. *B*, *in vitro* kinase assay. GST or the indicated GST-p73α deletion mutants bound to glutathione-Sepharose beads were washed with washing buffer and resuspended in 90 μl of kinase reaction buffer. Protein X, which was supplied by manufacturer, was used as a positive control. 10 μl of the active form of Plk1 were added to the reaction mixtures and incubated at 30 °C for 30 min. The reaction mixtures were washed with washing buffer and then incubated with 100 μl of polyclonal anti-phospho-Thr antibody at room temperature for 30 min followed by incubation with horseradish peroxidase-conjugated anti-rabbit IgG at room temperature for 30 min. After incubation, 100 μl of substrate reagent were added to the reaction mixtures and incubated at room temperature for 5 min. *Yellow* coloration indicates the Plk1-mediated phosphorylation at Thr residue. After the addition of 100 μl of stop solution, supernatant was transferred into 96-well tissue culture plate, and the absorbance reading was carried out at 450/540 nm using the microplate reader (*C*).

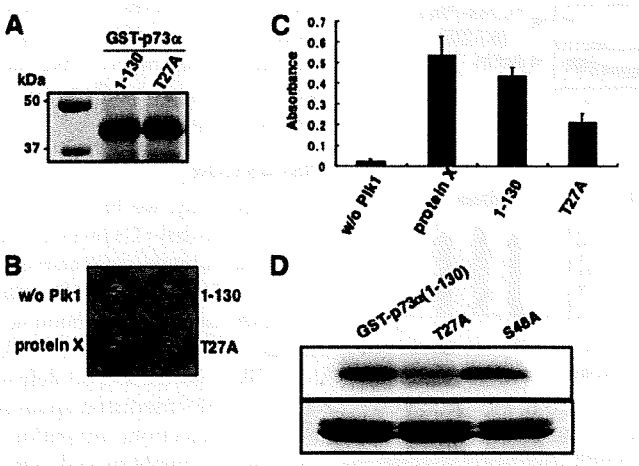

FIGURE 11. **Thr-27 of p73 is phosphorylated by Plk1 *in vitro*.** *A*, Coomassie Brilliant Blue staining of GST-p73α-(1–130) and the mutant form of GST-p73α-(1–130) termed T27A where Thr-27 was substituted to Ala. *B*, *in vitro* kinase assay. *In vitro* kinase reactions were performed using GST-p73α-(1–130) and T27A as described in Fig. 10*B*. *C*, absorbance reading of the *in vitro* kinase reactions. *D*, standard *in vitro* kinase assay. GST-p73α-(1–130), T27A, and S48A were incubated with the active form of Plk1 in the presence of [γ-^{32}P]ATP. The reaction mixtures were separated by SDS-PAGE and subjected to autoradiography (*top panel*). *Bottom panel* showed the Coomassie Brilliant Blue staining of the GST-p73α fusion proteins.

Plk1 bound to a DNA-binding domain of p53 and inhibited its transcriptional activity. For p73, Plk1 interacted with the region between NH_2-terminal transactivation domain and a DNA-binding domain of p73α, which includes the proline-rich domain (amino acid residues 81–113). Because NH_2-terminal proline-rich domain is involved in the transcriptional activity of p73 (34), it is possible that Plk1 masks the proline-rich domain to render p73α latent form. Thus, it is likely that Plk1-mediated inhibitory mechanisms of p73 is distinct from those of p53.

In response to CDDP, p73α as well as p53 is induced to accumulate in association with a down-regulation of Plk1 (20). Under our experimental conditions, Plk1 has an ability to promote a proteolytic degradation of p73 in a proteasome-independent manner. As described (35), calpain promoted the proteolytic cleavage of p73. However, our preliminary experiments demonstrated that the calpain inhibitor had an undetectable effect on Plk1-mediated proteolytic degradation of p73 (data not shown). Although the precise molecular mechanisms behind the Plk1-mediated proteolytic degradation of p73 remain unclear, our present results indicate that, under normal conditions, Plk1 might contribute to maintain pro-apoptotic p73 at extremely low levels and also suggest that Plk1-mediated proteolytic degradation of p73α might be an alternative molecular mechanism of p73 dysfunction. Similarly, Liu and Erikson (25) described that Plk1 depletion stabilizes p53 in HeLa cells. In support with this notion, Chen *et al.* (36) found that Plk1 inhibits UV-mediated phosphorylation of p53 at Ser-15 and thereby facilitates its nuclear export and proteolytic degradation.

As described (2, 3), p73 function is modulated by post-translational modifications such as phosphorylation and acetylation. Several lines of evidence suggest that phosphorylation of p73 does not always enhance its function (8–13). Based on our present results, Plk1 inhibited the p73α-mediated transcriptional activation, whereas the kinase-deficient mutant form of Plk1 did not, indicating that Plk1-dependent phosphorylation of p73 plays an inhibitory role in the regulation of p73 activity. In accordance with this notion, our *in vitro* kinase reactions demonstrated that GST-p73α-(1–130) is phosphorylated by Plk1. During the extensive search for putative phosphorylation site(s) within the NH_2-terminal portion of p73α, we found out two canonical phosphorylation sites targeted by Plk1, including (^{25}DSTYFD^{30}) and (^{46}DSSMDV^{51}). Thr-27 substituted to Ala

(T27A) resulted in a significant reduction of Plk1-mediated phosphorylation of GST-p73α-(1–130), whereas S48A mutant was efficiently phosphorylated by Plk1, suggesting that Thr-27 is at least one of the phosphorylation site(s) of p73α. Considering that Thr-27 exists within the transactivation domain of p73, it is likely that Plk1-mediated phosphorylation of p73α at Thr-27 might induce the conformational change of its transactivation domain and/or the dissociation of the co-activator such as p300/CBP from p73α, and thereby inhibiting transcriptional as well as pro-apoptotic activity of p73α. Indeed, Plk1 inhibited the complex formation between p73 and p300 (supplemental Fig. S5). In addition, it has been shown that p300-mediated acetylation of p73 increases the stability of p73 (15). Thus, it is possible that Plk1-mediated phosphorylation of p73 inhibits p73 function through the dissociation of p300 from p73 and also induces the degradation of latent forms of p73. Further studies should be required to address this issue.

Another finding of this study was that the endogenous Plk1 begins to accumulate in the cell nucleus in response to CDDP treatment. Based on our present results, Plk1 interacts with p73 and inhibits the apoptosis mediated by p73. Because the expression levels of Plk1 decreased in cells exposed to CDDP, p73 might be liberated from the inhibitory complex containing Plk1 to exert its pro-apoptotic activity. The precise molecular mechanisms behind the CDDP-induced nuclear accumulation of Plk1 remain unclear.

It has been well documented that the elevated levels of Plk1 expression show various human tumors (21, 37), and patients with tumors showed a clear correlation between lower survival rates and higher Plk1 expression levels (37–39). Taken together with our present and previous results (20), Plk1 has an ability to block the p53- and p73-dependent pro-apoptotic pathway, raising the possibility that Plk1 is one of the potential targets in cancer treatment.

Acknowledgment—We thank Y. Nakamura for technical assistance.

REFERENCES

1. Kaghad, M., Bonnet, H., Yang, A., Creancier, L., Biscan, J. C., Valent, A., Minty, A., Chalon, P., Lelias, J. M., Dumont, X., Ferrara, P., McKeon, F., and Caput, D. (1997) *Cell* **90,** 809–819
2. Melino, G., De Laurenzi, V., and Vousden, K. H. (2002) *Nat. Rev. Cancer* **2,** 605–615
3. Ozaki, T., and Nakagawara, A. (2005) *Cancer Sci.* **96,** 729–737
4. Bourdon, J. C., Fernandes, K., Murray-Zmijewski, F., Liu, G., Diot, A., Xirodiamas, D. P., Saville, M. K., and Lane, D. P. (2005) *Genes Dev.* **19,** 2122–2137
5. Stiewe, T., Zimmermann, S., Frilling, A., Esche, H., and Putzer, B. M. (2002) *Cancer Res.* **62,** 3598–3602
6. Pozniak, C. D., Radinovic, S., Yang, A., McKeon, F., Kaplan, D. R., and Miller, F. D. (2000) *Science* **289,** 304–306
7. Irwin, M., Kondo, K., Marin, M. C., Cheng, L. S., Hahn, W. C., and Kaelin, W. G., Jr. (2003) *Cancer Cell* **3,** 403–410
8. Gong, J., Costanzo, A., Yang, H.-Q., Melino, G., Kaelin, W. G., Jr., Levreno, M., and Wang, J. Y. (1999) *Nature* **399,** 806–809
9. Agami, R., Blandino, G., Oren, M., and Shaul, Y. (1999) *Nature* **399,** 809–813
10. Yuan, Z.-M., Shioya, H., Ishiko, T., Sun, X., Gu, J., Huang, Y. Y., Lu, H., Kharbanda, S., Weichselbaum, R., and Kufe, D. (1999) *Nature* **399,** 814–817
11. Ren, J., Datta, R., Shioya, H., Li, Y., Oki, E., Biedermann, V., Bharti, A., and Kufe, D. (2002) *J. Biol. Chem.* **277,** 33758–33765
12. Gonzalez, S., Prives, C., and Cordon-Cordo, C. (2003) *Mol. Cell. Biol.* **23,** 8161–8171
13. Gaiddon, C., Lokshin, M., Gross, I., Levasseur, D., Taya, Y., Loeffler, J.-P., and Prives, C. (2003) *J. Biol. Chem.* **278,** 27421–27431
14. Zeng, X., Li, X., Miller, A., Yuan, Z., Yuan, W., Kwok, R. P., Goodman, R., and Lu, H. (2000) *Mol. Cell. Biol.* **20,** 1299–1310
15. Costanzo, A., Merlo, P., Pediconi, N., Fulco, M., Sartorelli, V., Cole, P. A., Fontemaggi, G., Fanciulli, M., Schiltz, L., Blandino, G., Balsano, C., and Levrero, M. (2002) *Mol. Cell* **9,** 175–186
16. Barr, F. A., Sillje, H. H., and Nigg, E. A. (2004) *Nat. Rev. Mol. Cell Biol.* **5,** 429–440
17. Xie, S. Xie, B., Lee, M. Y., and Dai, W. (2005) *Oncogene* **24,** 277–286
18. Dai, W. (2005) *Oncogene* **24,** 214–216
19. Elia, A. E., Cantley, L. C., and Yaffe, M. B. (2003) *Science* **299,** 1228–1231
20. Ando, K., Ozaki, T., Yamamoto, H., Furuya, K., Hosoda, M., Hayashi, S., Fukuzawa, M., and Nakagawara, A. (2004) *J. Biol. Chem.* **279,** 25549–25561
21. Eckerdt, F., Yuan, J., and Strebhardt, K. (2005) *Oncogene* **24,** 267–276
22. Smith, M. R., Wilson, M. L., Hamanaka, R., Chase, D., Kung, H., Longo, D. L., and Ferris, D. K. (1997) *Biochem. Biophys. Res. Commun.* **234,** 397–405
23. Spankuch-Schmitt, B., Bereiter-Hahn, J., Kaufmann, M., and Strebhardt, K. (2002) *J. Natl. Cancer Inst.* **94,** 1863–1877
24. Spankuch-Schmitt, B., Wolf, G., Solbach, C., Loibl, S., Knecht, R., Stegmuller, M., von Minckwitz, G., Kaufmann, M., and Strebhardt, K. (2002) *Oncogene* **21,** 3162–3171
25. Liu, X., and Erikson, R. L. (2003) *Proc. Natl. Acad. Sci. U. S. A.* **100,** 5789–5794
26. Smits, V. A., Klompmaker, R., Arnaud, L., Rijksen, G., Nigg, E. A., and Medema, R. H. (2000) *Nat. Cell Biol.* **2,** 672–676
27. van Vugt, M. A., Smits, V. A., Klompmaker, R., Medema, R. H. (2001) *J. Biol. Chem.* **276,** 41656–41660
28. Liu, X., Lei, M., and Erikson, R. L. (2006) *Mol. Cell. Biol.* **26,** 2093–2108
29. Liu, Y., Shreder, K. R., Gai, W., Corral, S., Ferris, D. K., and Rosenblum, J. S. (2005) *Chem. Biol.* **12,** 99–107
30. Niizuma, T., Nakamura, Y., Ozaki, T., Nakanishi, H., Ohira, M., Isogai, E., Kageyama, H., Imaizumi, M., and Nakagawara, A. (2006) *Oncogene* **26,** 5046–5055
31. Hosoda, M., Ozaki, T., Miyazaki, K., Hayashi, S., Furuya, K., Watanabe, K., Nakagawa, T., Hanamoto, T., Todo, S., and Nakagawara, A. (2005) *Oncogene* **24,** 7156–7169
32. Zeng, X., Chen, L., Jost, C. A., Maya, R., Keller, D., Wang, X., Kaelin, W. G., Jr., Oren, M., Chen, J., and Lu, H. (1999) *Mol. Cell. Biol.* **19,** 3257–3266
33. Nakajima, H., Toyoshima-Morimoto, F., Taniguchi, E., and Nishida, E. (2003) *J. Biol. Chem.* **278,** 25277–25280
34. Tanaka, Y., Kameoka, M., Itaya, A., Ota, K., and Yoshihara, K. (2004) *Biochem. Biophys. Res. Commun.* **317,** 865–872
35. Munarriz, E., Bano, D., Sayan, A. E., Rossi, M., Melino, G., and Nicotera, P. (2005) *Biochem. Biophys. Res. Commun.* **333,** 954–960
36. Chen, J., Dai, G., Wang, Y. Q., Wang, S., Pan, F. Y., Xue, B., Zhao, D. H., and Li, C. J. (2006) *FEBS Lett.* **580,** 3624–3630
37. Takai, N., Hamanaka, R., Yoshimatsu, J., and Miyakawa, Y. (2005) *Oncogene* **24,** 287–291
38. Knecht, R., Elez, R., Oechler, M., Solbach, C., von Ilberg, C., and Strebhardt, K. (1999) *Cancer Res.* **59,** 2794–2797
39. Knecht, R., Oberhauser, C., and Strebhardt, K. (2000) *Int. J. Cancer* **89,** 535–536

Oncogene (2008) 27, 6075–6082

www.nature.com/onc

SHORT COMMUNICATION

N-MYC promotes cell proliferation through a direct transactivation of neuronal leucine-rich repeat protein-1 (*NLRR1*) gene in neuroblastoma

MS Hossain[1,2,5], T Ozaki[1,2,5], H Wang[1,3,5], A Nakagawa[4], H Takenobu[1], M Ohira[1], T Kamijo[1] and A Nakagawara[1,2]

[1]*Division of Biochemistry, Chiba Cancer Center Research Institute, Chiba, Japan;* [2]*Department of Molecular Biology and Oncology, Chiba University Graduate School of Medicine, Chiba, Japan;* [3]*Department of Pediatrics, ShengJing Hospital of China Medical University, Shenyang, People's Republic of China and* [4]*Department of Pathology, National Center for Child Health and Development, Tokyo, Japan*

Neuronal leucine-rich repeat protein-1 (*NLRR1*) gene encodes a type I transmembrane protein with unknown function. We have previously described that *NLRR1* gene is highly expressed in unfavorable neuroblastomas as compared with favorable tumors and its higher expression levels correlate significantly with poor clinical outcome. In this study, we have found that *NLRR1* gene is one of direct target genes for N-MYC and its gene product contributes to N-MYC-dependent growth promotion in neuroblastoma. Expression levels of *NLRR1* were significantly associated with those of N-*MYC* in various neuroblastoma cell lines as well as primary neuroblastoma tissues. Indeed, enforced expression of N-MYC resulted in a remarkable induction of the endogenous *NLRR1*. Consistent with these results, we have identified two functional E-boxes within the promoter region and intron 1 of *NLRR1* gene. Intriguingly, c-myc also transactivated *NLRR1* gene. Enforced expression of NLRR1 promoted cell proliferation and rendered cells resistant to serum deprivation. In support with these observations, small-interfering RNA-mediated knockdown of the endogenous *NLRR1*-reduced growth rate and sensitized cells to serum starvation. Collectively, our present findings provide a novel insight into understanding molecular mechanisms behind aggressive neuroblastoma with N-*MYC* amplification.
Oncogene (2008) **27,** 6075–6082; doi:10.1038/onc.2008.200; published online 30 June 2008

Keywords: c-myc; neuroblastoma; N-MYC; NLRR1; proliferation; transactivation

In a sharp contrast to c-*myc*, the expression of N-*MYC* is largely restricted to embryonic tissues and neuroendocrine tumors (Boon *et al.*, 2001). It has been established that N-*MYC* gene amplification is strongly associated with poor clinical outcome of aggressive human neuroblastoma (Kohl *et al.*, 1983; Schwab *et al.*, 1983; Seeger *et al.*, 1985). Indeed, enforced expression of N-*MYC* in neuroblastoma cell lines resulted in an accelerated proliferation (Bernards *et al.*, 1986; Lutz *et al.*, 1996), whereas treatment of neuroblastoma cells with antisense oligonucleotides specific to N-*MYC* decreased their proliferation (Negroni *et al.*, 1991). Consistent with these observations, transgenic mice overexpressing N-*MYC* in neural crest-derived tissues displayed frequent development of neuroblastomas (Weiss *et al.*, 1997), suggesting that deregulated expression of N-MYC is causative in genesis and development of neuroblastoma *in vivo*. However, it is still unclear how N-MYC contributes to the formation of neoplastic phenotypes of neuroblastoma.

N-MYC is a nuclear transcription factor containing NH_2-terminal transactivation domain and COOH-terminal helix-loop-helix/leucine-zipper domain as well as the basic region (Kouzarides and Ziff, 1988; Landschulz *et al.*, 1988; Murre *et al.*, 1989). N-MYC forms a heterodimeric complex with Max through their helix-loop-helix/leucine-zipper domains and binds to consensus site known as E-box (CACGTG) (Alex *et al.*, 1992; Blackwood *et al.*, 1992; Torres *et al.*, 1992). Identification of its direct transcriptional target gene(s) might provide a novel insight into understanding the functional contribution of N-MYC in malignant phenotypes of aggressive neuroblastoma. Extensive efforts demonstrated that prothymosin-α, ornithine decarboxylase teromerase reverse transcriptase, *Id2* and genes involved in ribosome biogenesis are transcriptional targets of N-MYC (Lutz *et al.*, 1996; Wang *et al.*, 1998; Lasorella *et al.*, 2000; Boon *et al.*, 2001). Recently, Slack *et al.* (2005) described that MDM2 that acts as an E3 ubiquitin protein ligase for tumor suppressor, p53, is a putative transcriptional target of N-MYC. According to their results, N-MYC directly binds to a consensus E-box within human *MDM2* promoter region and N-MYC has an ability to transactivate *MDM2* promoter. Furthermore, the endogenous MDM2 increased in N-MYC-inducible neuroblastoma cells. These observations suggest that MDM2 is important in N-MYC-driven neuroblastoma development.

Correspondence: Dr A Nakagawara, Division of Biochemistry, Chiba Cancer Center Research Institute, 666-2 Nitona, Chuoh-ku, Chiba 260-8717, Japan.
E-mail: akiranak@chiba-cc.jp
[5]These authors contributed equally to this work.
Received 28 February 2008; revised 30 April 2008; accepted 22 May 2008; published online 30 June 2008

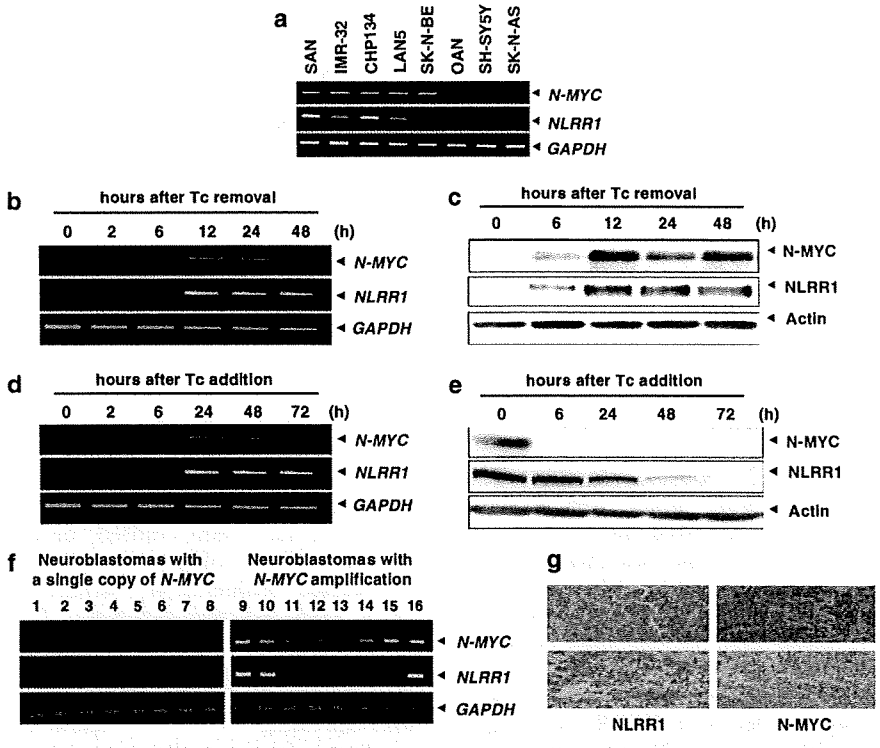

Figure 1 Expression of N-*MYC* and neuronal leucine-rich repeat protein-1 (*NLRR1*) in various neuroblastoma-derived cell lines and primary tissues. (a) Expression of *NLRR1* is restricted in neuroblastoma cell lines with N-*MYC* amplification. Total RNA was prepared from neuroblastoma cell lines with N-*MYC* amplification (SAN, IMR-32, CHP134, LAN5 and SK-N-BE) and neuroblastoma cell lines bearing a single copy of N-*MYC* (OAN, SH-SY5Y and SK-N-AS) using RNeasy Mini Kit (Qiagen, Valencia, CA, USA) and analysed for expression levels of N-*MYC* (top) and *NLRR1* (middle) by reverse transcription (RT) PCR. *GAPDH* was used as an internal control (bottom) The oligonucleotide primer sequences used in this study are as follows: human *NLRR1*, 5′-GTCGATGTCCATGAATACAACCT-3′ (sense) and 5′-CAAGGCTAATGACGGCAAAC-3′ (antisense); human *N-MYC*, 5′-CTTCGGTCCAGCTTTCTCAC-3′ (sense) and 5′-GTCCGAGCGTGTTCAATTTT-3′ (antisense); human *GAPDH*, 5′-ACCTGACCTGCCGTCTAGAA-3′ (sense) and 5′-TCCACCACCCTGTTGCTGTA-3′ (antisense). (b, c) Induction of NLRR1 in N-*MYC*-inducible Tet21N cells. At the indicated time points after removal of tetracycline (Tc), total RNA and cell lysates were prepared and processed for RT PCR (b) and immunoblotting with anti-N-MYC (Ab-1, Oncogene Research Products, Cambridge, MA, USA), anti-NLRR1 and anti-actin (20 33, Sigma, St Louis, MO, USA) antibodies (c), respectively. For RT PCR, *GAPDH* was used as an internal control. For immunoblotting, actin was used as a loading control. (d, e) Downregulation of NLRR1 in Tet21N cells maintained in the presence of Tc. At the indicated time periods after the addition of Tc (100 ng/ml), total RNA and cell lysates were prepared and subjected to RT PCR (d) and immunoblotting (e), respectively. (f) Expression of *NLRR1* in primary neuroblastomas. Total RNA was prepared from eight favorable neuroblastomas (cases 1 8) and eight unfavorable ones (cases 9 16) and subjected to RT PCR to examine expression levels of N-*MYC* (top) and *NLRR1* (middle). *GAPDH* was used as an internal control (bottom). (g) Immunohistochemical analysis. Primary neuroblastomas tissues with *N-MYC* amplification were immunostained with anti-NLRR1 (left panels) or with anti-N-MYC antibody (right panels). The BenchMark XT immunostainer (Ventana Medical Systems, Tucson, AZ, USA) and 3,3′ diaminobenzidine detection kit (Ventana Medical Systems) were used to visualize NLRR1 and N-MYC. All patients agreed to participate and provided written informed consent and our present study was approved by institutional ethical review committee.

Mammalian neuronal leucine-rich repeat protein family (NLRR) is a type I transmembrane protein with extracellular leucine-rich repeats, which is composed of NLRR1-5 (Taguchi *et al*., 1996; Taniguchi *et al*., 1996; Hamano *et al*., 2004; Bando *et al*., 2005). NLRR proteins have been proposed to function as cell adhesion or signaling molecules (Fukamachi *et al*., 2002). We have previously reported that expression levels of *NLRR1* are significantly higher in unfavorable neuroblastoma than those in favorable one and higher expression levels of *NLRR1* closely correlate with poor clinical outcome of patients with neuroblastoma (Hamano *et al*., 2004). In contrast, *NLRR3* and *NLRR5* were expressed at higher levels in favorable neuroblastoma as compared with unfavorable one. For *NLRR2*, no significant differences were observed in its expression levels between favorable and unfavorable neuroblastomas (Hamano *et al*., 2004). In the present study, we have found that *NLRR1* is a direct transcriptional target of N-MYC and its gene product is important in the regulation of neuroblastoma cell proliferation.

To examine a possible correlation between expression levels of N-*MYC* and *NLRR1* in neuroblastoma cells, total RNA was prepared from the indicated cell lines and subjected to reverse transcription (RT)–PCR. As shown in Figure 1a, all neuroblastoma cell lines

with N-*MYC* amplification that we examined expressed *NLRR1* mRNA, whereas we did not detect *NLRR1* mRNA in OAN, SH-SY5Y and SK-N-AS cells bearing a single copy of N-*MYC* under our experimental conditions. To confirm a possible relationship between N-*MYC* and *NLRR1*, we employed N-*MYC*-inducible neuroblastoma cells (Tet21N) derived from parental neuroblastoma cell line SHEP (Lutz *et al.*, 1996). According to their results, Tet21N cells constitutively expressed N-*MYC* in the absence of tetracycline (Tc), whereas the addition of Tc to the culture decreased N-*MYC* expression levels. For this purpose, we have generated polyclonal antibody against NLRR1 that recognizes the region including amino-acid residues between positions 693 and 712. At the indicated time points after Tc depletion, total RNA and cell lysates were prepared and subjected to RT–PCR and immunoblotting, respectively. As shown in Figure 1b, Tc deprivation led to an induction of N-*MYC* in association with a significant increase in expression levels of *NLRR1*. Similar results were also obtained in immunoblotting analysis (Figure 1c). In contrast to the withdrawal of Tc, the addition of Tc to the culture significantly reduced expression levels of N-*MYC* and the concomitant decrease in expression levels of *NLRR1* was detectable at mRNA and protein levels (Figures 1d and e), suggesting that *NLRR1* might be a direct transcriptional target of N-MYC.

Consistent with these results, *NLRR1* expression was undetectable in favorable primary neuroblastomas carrying a single copy of N-*MYC*, whereas unfavorable primary neuroblastomas bearing N-*MYC* amplification expressed substantial amounts of *NLRR1* (Figure 1f). Immunohistochemical analyses also revealed that NLRR1 is coexpressed with N-MYC in primary neuroblastomas bearing N-*MYC* amplification (Figure 1g). On the other hand, NLRR1 was undetectable in primary neuroblastomas carrying a single copy of *N-MYC* (data not shown). In addition, Spearman's rank correlation coefficient between *NLRR1* and *MYCN* mRNA expression in 136 primary neuroblastomas was 0.42 ($P<0.0001$) as shown in the scatter plot of Supplementary Figure S1, suggesting that *NLRR1* and *MYCN* expression in primary tumors is also positively correlated.

To address whether N-MYC could enhance the transcription of *NLRR1*, HeLa cells were transfected with or without the increasing amounts of the expression plasmid encoding N-MYC. As clearly shown in Supplementary Figure S2, N-MYC had an ability to transactivate the endogenous *NLRR1* in a dose-dependent manner. In contrast, N-MYC had undetectable effects on expression levels of the endogenous *NLRR2* (data not shown). Intriguingly, c-myc was also capable to transactivate the endogenous *NLRR1* (Supplementary Figure S2). Expression levels of *cyclin* E were examined as a positive control. As it has been well established that N-MYC recognizes and binds to so-called E-box (5′-CACGTG-3′), we sought to find out the putative E-box sequence(s) within 5′-upstream region as well as intron 1 of *NLRR1* gene. Finally, we found out three (E-1, E-2 and E-3) and two candidate E-boxes (E-4 and E-5) within 5′-upstream region and intron 1 of *NLRR1* gene, respectively (Figure 2a). To investigate whether these canonical E-boxes could respond to N-MYC, we subcloned genomic fragments containing each of these putative E-boxes into luciferase reporter plasmid to give pluc-E1, pluc-E2, pluc-E3, pluc-E4 and pluc-E5. SK-N-AS cells carrying a single copy of N-*MYC* were co-transfected with the constant amount of the expression plasmid for N-MYC and *Renilla* luciferase reporter plasmid together with the indicated luciferase reporter plasmids. At 48 h after transfection, cells were lysed and their luciferase activities were measured. As shown in Figure 2b, E-1 and E-4 boxes showed the relatively higher luciferase activities than those of the remaining putative E-box-containing fragments. Similar results were also obtained in mouse neuroblastoma Neuro2a cells (data not shown). Thus, we focused our attention on E-1 and E-4 boxes. To verify the functional significance of E-1 and/or E4 box, we have disrupted E-1 or E-4 box to give pluc-E1Δ or pluc-E4Δ luciferase reporter construct. Luciferase reporter assays demonstrated that pluc-E1Δ and pluc-E4Δ do not respond to exogenously expressed N-MYC (Figure 2c). These results indicate that E-1 and E-4 boxes are the functional elements involved in N-MYC-dependent transcriptional activation of *NLRR1*.

To ask whether N-MYC could be recruited onto E-1 and/or E-4 box in cells, we performed chromatin immunoprecipitation (ChIP) assays. Cross-linked chromatin prepared from the indicated cells was immunoprecipitated with normal mouse serum or with monoclonal anti-N-MYC antibody. Under our experimental conditions, an average length of sonicated genomic DNA fragments was 200–800 nucleotides in length (data not shown). The genomic DNA was purified from immunoprecipitates and amplified by PCR. As shown in Figure 2d, the estimated sizes of PCR products containing E-1 or E-4 box were detectable in IMR-32, SAN and CHP134 cells with N-*MYC* amplification, whereas our ChIP assays did not detect the estimated PCR products in SK-N-AS and SH-SY5Y cells bearing a single copy of N-*MYC*. In addition, we could not detect the efficient recruitment of N-MYC onto E-3 box that did not respond to exogenously expressed N-MYC. Consistent with these results, the anti-N-MYC immunoprecipitates prepared from Tet21N cells maintained in the absence of Tc contained the genomic fragments encompassing E-1 and E-4 boxes. In a sharp contrast, genomic fragment including E-3 box was not detectable in the anti-N-MYC immunoprecipitates prepared from Tet21N cells cultured in the absence of Tc. These observations suggest that N-MYC is recruited onto E-1 and E-4 boxes of *NLRR1* gene in cells.

We next examined a possible effect of NLRR1 on cell growth of neuroblastoma cells. SK-N-BE cells were transfected with the empty plasmid or with the expression plasmid for Myc-tagged NLRR1 (NLRR1-Myc). At 48 h after transfection, cells were transferred into fresh medium containing G418 for 2 weeks.

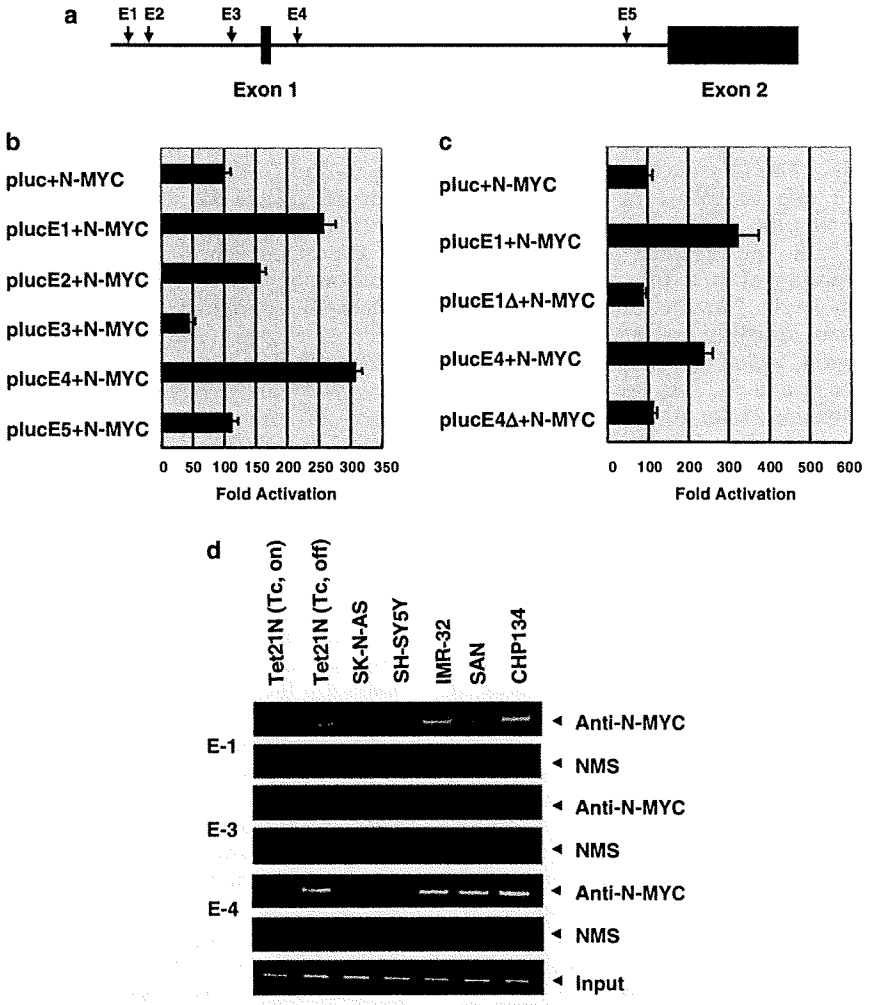

Figure 2 Luciferase reporter analysis. (a) Schematic drawing of the 5′-upstream region and intron 1 of human Neuronal leucine-rich repeat protein-1 (*NLRR1*) gene. Exons 1 and 2 were indicated by solid boxes. The positions of putative E-boxes were indicated by arrows. (b) Luciferase reporter assays. SK-N-AS cells were co-transfected with the constant amount of N-MYC-expression plasmid (100 ng), *Renilla* luciferase reporter plasmid (pRL-TK, 10 ng) and luciferase reporter plasmid containing E-1, E-2, E-3, E-4 or E-5 box (100 ng). Total amount of plasmid DNA per transfection was kept constant (510 ng) with pcDNA3. At 48 h after transfection, cells were lysed and their luciferase activities were measured by Dual-Luciferase reporter system (Promega, Madison, WI, USA). The firefly luminescence signal was normalized based on the *Renilla* luminescence signal. The results were obtained at least three independent experiments. (c) E-1 and E-4 boxes are required for N-MYC-dependent transactivation of *NLRR1* promoter. SK-N-AS cells were co-transfected with the constant amount of the expression plasmid for N-MYC (100 ng), pRL-TK (10 ng) and luciferase reporter plasmid lacking E-1 (pluc-E1Δ) or E-4 box (pluc-E4Δ). At 48 h after transfection, cells were lysed and their luciferase activities were measured as in (b). (d) N-MYC is efficiently recruited onto E-1 and E-4 boxes. Chromatin immunoprecipitation (ChIP) assays were carried out using chromatin immunoprecipitation assay kit provided from Upstate (Charlottesville, VA, USA). In brief, the indicated cells were cross-linked with formaldehyde and cross-linked chromatin was sonicated followed by immunoprecipitation with normal mouse serum (NMS) or with monoclonal anti-N-MYC antibody. Genomic DNAs were purified from the immunoprecipitates and subjected to PCR to amplify the genomic region containing E-1, E-3 and E-4 boxes. The oligonucleotide primer sequences used in this study are as follows: E-1, 5′-AAGTTGGATTTGATGACTGATACG-3′ (sense) and 5′-AGGCAAGAGACCATGTGCAGGAG-3′ (antisense); E-3, 5′-ATGAATCGAACAGTGGAGAGAC-3′ (sense) and 5′-AATGCTTAGGACAGTGCTTAG-3′ (antisense); E-4, 5′-TGTCTA ACATTAGCTGCGTGACC-3′ (sense) and 5′-AATGCTGTTCCGTGAATAGGTTC-3′ (antisense).

Drug-resistant cells were collected and their growth was examined. As shown in Figure 3a, exogenous NLRR1-Myc was expressed in drug-resistant cells transfected with NLRR1-Myc expression plasmid. Of note, NLRR1-Myc transfectants displayed an accelerated proliferation as compared with the control transfectants ($P<0.01$; Figure 3b). To investigate the possible role of the endogenous NLRR1, we have designed small-interfering RNA (siRNA) against NLRR1. As shown in Figure 3c, siRNA-targeting NLRR1 significantly downregulated the expression levels of the endogenous NLRR1 in SK-N-BE cells. As expected, siRNA-mediated knockdown of the endogenous NLRR1 significantly reduced the rate of cell growth as compared

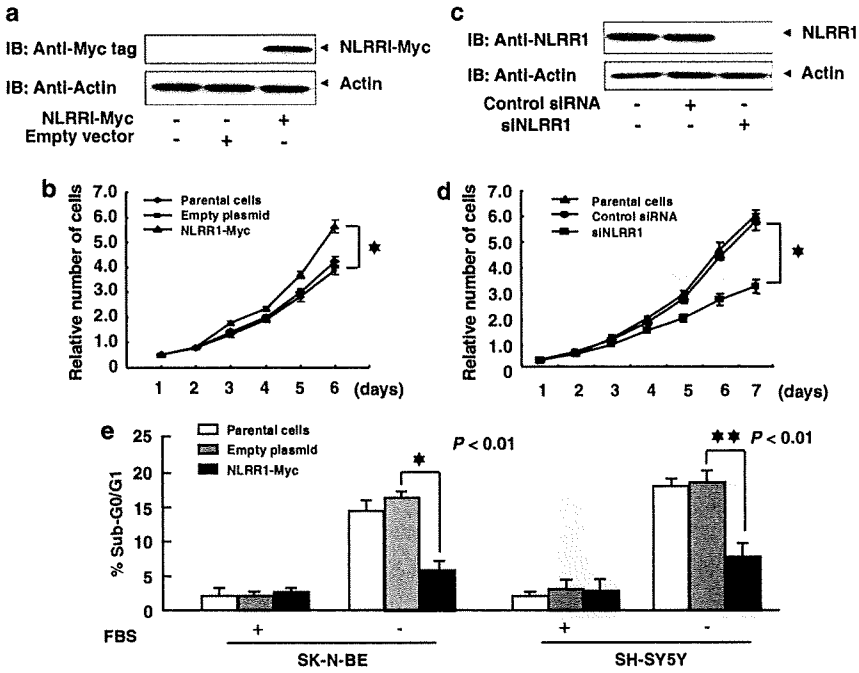

Figure 3 Neuronal leucine-rich repeat protein-1 (NLRR1) promotes cell proliferation. (**a**) Exogenous expression of NLRR1-Myc in SK-N-BE cells. SK-N-BE cells were transfected with the empty plasmid or with the expression plasmid for Myc-tagged NLRR1 (NLRR1-Myc) using Lipofectamine 2000 transfection reagent (Invitrogen, Carlsbad, CA, USA). At 48 h after transfection, cells were transferred into fresh medium containing G418 (600 μg/ml). After 2 weeks of selection, drug-resistant cells were harvested and analysed for the expression of exogenous NLRR1-Myc by immunoblotting with anti-Myc tag (PL14, Medical & Biological Laboratories, Nagoya, Japan) antibody. (**b**) Growth curves. Parental cells, control transfectants and NLRR1-Myc transfectants were seeded at a density of 1×10^5 cells per cell culture dish and allowed to attach overnight (day 1). At the indicated time points after seeding the cells, number of viable cells were measured and presented by graphs. Solid diamonds, squares and triangles indicate parental cells, control and NLRR1-Myc transfectants, respectively. $^*P<0.01$. (**c**) Small-interfering RNA (siRNA)-mediated knockdown of the endogenous NLRR1. SK-N-BE cells were transfected with control siRNA or with siRNA against NLRR1 (20 nM, Takara, Ohtsu, Japan) using Lipofectamine RNAiMAX (Invitrogen). At 48 h after transfection, cell lysates were prepared and subjected to immunoblotting with anti-NLRR1 antibody. (**d**) Growth curves. SK-N-BE cells were transfected as in (**c**). At 24 h after transfection, attached cells were collected and seeded at a density of 1×10^5 cells per cell culture plates. At the indicated time points after seeding the cells, number of viable cells were measured and presented by graphs. Solid triangles, circles and squares indicate parental cells, control transfectants and NLRR1-knocked down cells, respectively. $^*P<0.01$. (**e**) NLRR1 has an anti-apoptotic potential in response to fetal bovine serum (FBS) starvation. SK-N-BE and SH-SY5Y cells were transfected with the empty plasmid or with the expression plasmid encoding NLRR1-Myc. At 48 h after transfection, cells were transferred into fresh medium containing G418 (600 μg/ml). After 2 weeks of selection, drug-resistant cells were harvested and cultured in the presence or absence of FBS. At 24 h after treatment, floating and attached cells were collected, stained with propidium iodide (PI) and their cell-cycle distributions were analysed by fluorescence-activated cell sorting (FACS, Becton Dickinson, Mountain View, CA, USA). Results obtained by FACS analysis were presented by graphs. Open, gray and solid boxes indicate parental cells, control transfectants and NLRR1-Myc-expressing transfectants, respectively. $^*P<0.01$, $^{**}P<0.01$.

with the control cells ($P<0.01$; Figure 3d), indicating that NLRR1 has an ability to promote cell growth in neuroblastoma.

As described previously (Hamano *et al*., 2004), *NLRR1* was expressed at significantly higher levels in unfavorable neuroblastoma than favorable one, indicating that NLRR1 might have an anti-apoptotic activity. To address this issue, SK-N-BE and SH-SY5Y cells were transfected with the empty plasmid or with the expression plasmid for NLRR1-Myc. At 48 h after transfection, cells were exposed to G418 for 2 weeks. Drug-resistant cells were collected and cultured in the presence or absence of fetal bovine serum (FBS). At 24 h after FBS starvation, floating and attached cells were harvested, stained with propidium iodide and measured number of cells with sub-G_0/G_1 DNA content by fluorescence-activated cell sorting (FACS) analysis. As shown in Figure 3e, FBS deprivation increased number of parental and control SK-N-BE cells with sub-G_0/G_1 DNA content as compared with those cultured in the presence of FBS, whereas enforced expression of NLRR1-Myc significantly decreased number of cells with sub-G_0/G_1 DNA content relative to parental and control cells under FBS deprivation. Similar results were also obtained in SH-SY5Y cells (Figure 3e).

In support with these results, cleaved caspase-3 was detectable in control SK-N-AS transfectants maintained in the absence of FBS, whereas we did not detect cleaved caspase-3 in NLRR1-Myc transfectants under FBS deprivation (Figure 4a). Cleaved caspase-3 was also detected in parental cells in the absence of FBS (Figure 4b). In addition, cleaved poly-(ADP-ribose)

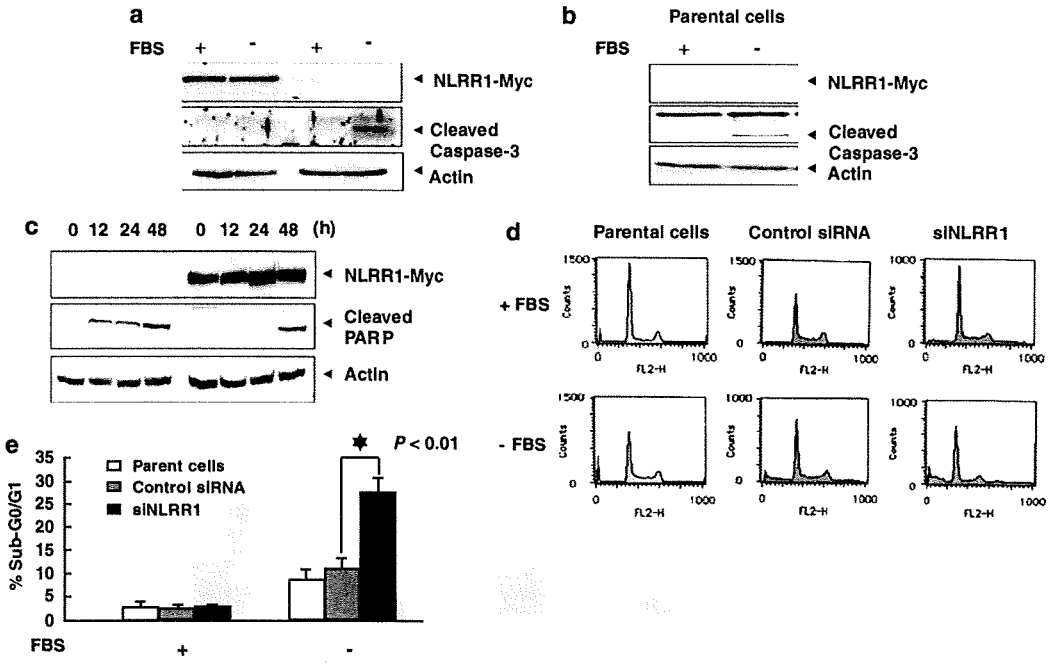

Figure 4 Neuronal leucine-rich repeat protein-1 (NLRR1) is involved in the regulation of serum starvation-induced apoptosis. (**a**) NLRR1 inhibits the activation of caspase-3. Control transfectants and NLRR1-Myc-expressing transfectants derived from SK-N-AS cells were cultured in the presence or absence of fetal bovine serum (FBS). At 24 h after the treatment, cell lysates were prepared and processed for immunoblotting with anti-Myc tag (top) or with anti-caspase-3 (Cell Signaling, Beverly, MA, USA) antibody (middle). Actin was used as a loading control (bottom). (**b**) Deprivation of FBS induces cleavage of caspase-3 in SK-N-AS cells. SK-N-AS cells were cultured in the presence or in the absence of FBS. At 24 h after the treatment, cell lysates were prepared and subjected to immunoblotting with the indicated antibodies. (**c**) Effect of NLRR1 on cleavage of poly-(ADP-ribose) polymerase (PARP) in response to FBS deprivation. Control transfectants (left) and NLRR1-Myc-expressing transfectants (right) were maintained in the absence of FBS. At the indicated time points after FBS withdrawal, cell lysates were prepared and analysed for the expression of NLRR1-Myc (top) as well as the proteolytic cleavage of PARP by immunoblotting with anti-PARP (Cell Signaling) antibody (middle). Actin was used as a loading control (bottom). (**d**, **e**) Small-interfering RNA (siRNA)-mediated knockdown of the endogenous NLRR1 enhances apoptosis in response to FBS starvation. Tet21N cells were grown in the fresh medium without tetracycline (Tc) and transfected with control siRNA or with siRNA against NLRR1. At 48 h after transfection, cells were transferred into fresh medium without Tc and FBS. At 24 h after FBS starvation, floating and attached cells were collected, stained with propidium iodide (PI) and their cell-cycle distributions were examined by fluorescence-activated cell sorting (FACS) (**d**). Results obtained by FACS analysis were presented by graphs. Open, gray and solid boxes indicate parental cells, control transfectants and NLRR1-knocked down transfectants, respectively (e). $^*P<0.01$.

polymerase (PARP) that is one of caspase-3 substrates (Truscott *et al.*, 2007), started to be observed in control transfectants 12 h after FBS starvation (Figure 4c). On the other hand, the kinetics for cleavage of PARP was delayed in NLRR1-Myc transfectants. Under our experimental conditions, control SK-N-AS transfectants underwent apoptosis in response to FBS deprivation, whereas enforced expression of NLRR1-Myc in SK-N-AS cells inhibited the FBS deprivation-induced apoptosis (data not shown). These findings suggest that NLRR1 confers resistance of neuroblastoma cells to FBS starvation-induced apoptosis.

To further confirm this notion, Tet21N cells were maintained in the absence of Tc and then transfected with control siRNA or with siRNA against NLRR1. At 48 h after transfection, cells were cultured in the absence of FBS for 24 h and then their cell-cycle distributions were analysed by FACS. As shown in Figures 4d and e, siRNA-mediated knockdown of the endogenous NLRR1 resulted in a significant increase in number of cells with sub-G_0/G_1 DNA content in response to FBS deprivation as compared with parental cells and control transfectants. Collectively, our present results strongly suggest that NLRR1 is a novel transcriptional target of N-MYC and has a growth-promoting as well as anti-apoptotic potential.

Small-interfering RNA-mediated knockdown of the endogenous NLRR1 in SK-N-BE cells bearing N-*MYC* amplification resulted in a significant decrease in the rate of cell growth. Furthermore, enforced expression of NLRR1-Myc conferred resistance of SK-N-BE and SH-SY5Y cells to FBS deprivation-mediated apoptosis. In contrast, siRNA-mediated knockdown of the endogenous NLRR1 led to an increase in number of cells with sub-G_0/G_1 DNA content in response to FBS deprivation. In addition, NLRR1-Myc blocked the activation of caspase-3 in SK-N-AS cells exposed to FBS depletion and thereby inhibiting the proteolytic cleavage of PARP. Thus, it is conceivable that NLRR1 inhibits the mitochondria-dependent intrinsic apoptotic pathway of caspase activation (Degterev *et al.*, 2003). As

reported previously (Hamano *et al.*, 2004), expression levels of *NLRR1* in unfavorable neuroblastoma were significantly higher than those of favorable one and closely correlated with poor clinical outcome. As aggressive neuroblastoma displays unfavorable clinical outcome despite intensive chemotherapy (Brodeur and Nakagawara, 1992), it is likely that N-MYC-mediated induction of NLRR1 is involved in the regulation of chemoresistant phenotypes of certain neuroblastomas. However, precise molecular mechanisms behind NLRR1-mediated growth promotion and anti-apoptotic effect in response to FBS starvation remain unclear. Further studies should be necessary to address this issue.

According to our present results, N-MYC-dependent transcriptional induction of *NLRR1* was observed in neuroblastoma cell lines. Furthermore, expression levels of *NLRR1* significantly correlated with those of N-*MYC* in primary neuroblastomas. Intriguingly, the enforced expression of N-MYC in HeLa cells also induced the expression of NLRR1, indicating that N-MYC-mediated transcriptional activation of *NLRR1* is not restricted to neuroblastoma cells. As described previously (Blackwood and Eisenman, 1991; Torres *et al.*, 1992), c-myc/Max heterodimeric complex also recognizes and binds to E-box. Like N-MYC, c-myc had an ability to induce the expression of NLRR1. Of note, our luciferase reporter assays indicated that E-1 and E-4 boxes are required for N-MYC-dependent activation of *NLRR1* promoter, whereas E-3 box does not respond to N-MYC. Similar results were also obtained in cells transfected with the expression plasmid for c-myc (data not shown). As described previously (Hamano *et al.*, 2004), *NLRR1* was expressed ubiquitously in human tissues. Among them, higher levels of *NLRR1* expression were observed in nerve tissues. Considering that N-*MYC* expression is largely restricted to embryonic tissues as well as neuroendocrine tumors, whereas c-*myc* is expressed in a wide variety of tissues as well as tumors (Boon *et al.*, 2001), N-MYC and c-myc might act as transcription factors for *NLRR1* in a cell-type-dependent manner under physiological conditions.

In the present study, we have found that *NLRR1* is one of direct transcriptional targets of oncogenic N-MYC and is important in the regulation of cell proliferation and the protection of cells from FBS deprivation-induced apoptosis in neuroblastoma cells. In support with this notion, there exists a positive correlation between expression levels of N-*MYC* and *NLRR1* in primary neuroblastomas. To our knowledge, NLRR1 is a first membrane protein whose expression levels are directly regulated by N-MYC. Thus, our present findings might provide a novel insight into understanding molecular mechanisms behind genesis and development of aggressive neuroblastoma with N-*MYC* amplification.

Acknowledgements

We are grateful to Dr M Schwab for providing the expression plasmid for N-MYC. We thank Ms Y Nakamura for technical assistance. This work was supported in part by a Grant-in-Aid from the Ministry of Health, Labour and Welfare for Third Term Comprehensive Control Research for Cancer, a Grant-in-Aid for Scientific Research on Priority Areas from the Ministry of Education, Culture, Sports, Science and Technology, Japan, a Grant-in-Aid for Scientific Research from Japan Society for the Promotion of Science, Uehara Memorial Foundation and Hisamitsu Pharmaceutical Co.

References

Alex R, Sozeri O, Meyer S, Dildrop R. (1992). Determination of the DNA sequence recognized by the bHLH-zip domain of the N-Myc protein. *Nucleic Acids Res* **20**: 2257 2263.

Bando T, Sekine K, Kobayashi S, Watabe AM, Rump A, Tanaka M *et al.* (2005). Neuronal leucine-rich repeat protein 4 functions in hippocampus-dependent long-lasting memory. *Mol Cell Biol* **25**: 4166 4175.

Bernards R, Dessain SK, Weinberg RA. (1986). N-myc amplification causes down-modulation of MHC class I antigen expression in neuroblastoma. *Cell* **47**: 667 674.

Blackwood EM, Eisenman RN. (1991). Max: a helix-loop-helix zipper protein that forms a sequence-specific DNA binding complex with Myc. *Science* **251**: 1211 1217.

Blackwood EM, Kretzner I, Eisenman RN. (1992). Myc and Max function as a nucleoprotein complex. *Curr Opin Genet Dev* **2**: 227 235.

Boon K, Caron HN, van Asperen R, Valentijn L, Hermus MC, van Sluis P *et al.* (2001). N-myc enhances the expression of a large set of genes functioning ribosome biogenesis and protein synthesis. *EMBO J* **20**: 1383 1393.

Brodeur GM, Nakagawara A. (1992). Molecular basis of clinical heterogeneity in neuroblastoma. *Am J Pediatr Hematol Oncol* **14**: 111 116.

Degterev A, Boyce M, Yuan J. (2003). A decade of caspases. *Oncogene* **22**: 8543 8567.

Fukamachi K, Matsuoka Y, Ohno H, Hamaguchi T, Tsuda H. (2002). Neuronal leucine-rich repeat protein-3 amplifies MAPK activation by epidermal growth factor through a carboxyl-terminal region containing endocytosis motifs. *J Biol Chem* **277**: 43549 43552.

Hamano S, Ohira M, Isogai E, Nakada K, Nakagawara A. (2004). Identification of novel human neuronal leucine-rich repeat (h*NLRR*) family, genes and inverse association of expression of *Nbla10449*/h*NLRR-1* and *Nbla10677*/h*NLRR-3* with the prognosis of primary neuroblastomas. *Int J Oncol* **24**: 1457 1466.

Kohl NE, Kanda N, Schreck RR, Bruns G, Latt SA, Gilbert F *et al.* (1983). Transposition and amplification of oncogene-related sequences in human neuroblastomas. *Cell* **35**: 359 367.

Kouzarides T, Ziff E. (1988). The role of the leucine zipper in the fos-jun interaction. *Nature* **336**: 646 651.

Landschulz WH, Johnson PF, McKnight S. (1988). The leucine zipper: a hypothetical structure common to a new class of DNA binding proteins. *Science* **240**: 1759 1764.

Lasorella A, Noseda M, Beyna M, Iavarone A. (2000). Id2 is a retinoblastoma protein target and mediates signaling by Myc oncoproteins. *Nature* **407**: 592 598.

Lutz W, Stohr M, Schurmann J, Wenzel A, Lohr A, Schwab M. (1996). Conditional expression of N-myc in human neuroblastoma cells increases expression of a-prothymosin and ornithine decarboxylase and accelerates progression into S-phase early after mitogenic stimulation of quiescent cells. *Oncogene* **13**: 803 812.

Murre C, Schonleber McCaw P, Baltimore D. (1989). A new DNA binding and dimerization motif in immunoglobulin enhancer binding, daughterless, MyoD, and myc proteins. *Cell* **56**: 777 783.

Negroni A, Scarpa S, Romeo A, Ferrari S, Modesti A, Raschella G. (1991). Decrease of proliferation rate and induction of differentiation by a MYCN antisense DNA oligomer in a human neuroblastoma cell line. *Cell Growth Differ* **2**: 511 518.

Schwab M, Alitalo K, Klempnauer KH, Varmus HE, Bishop JM, Gilbert F *et al.* (1983). Amplified DNA with limited homology to *myc* cellular oncogene is shared by human neuroblastoma cell lines and a neuroblastoma tumour. *Nature* **305**: 245 248.

Seeger RC, Brodeur GM, Sather H, Dalton A, Siegel SE, Wong KY *et al.* (1985). Association of multiple copies of the N-myc oncogene with rapid progression of neuroblastomas. *N Engl J Med* **313**: 1111 1116.

Slack A, Chen Z, Tonelli R, Pule M, Hunt L, Pession A *et al.* (2005). The p53 regulatory gene MDM2 is a direct transcriptional target of MYCN in neuroblastoma. *Proc Natl Acad Sci USA* **102**: 731 736.

Taguchi A, Wanaka A, Mori T, Matsumoto K, Imai Y, Takagi T *et al.* (1996). Molecular cloning of novel leucine-rich repeat proteins and their expression in the developing mouse nervous system. *Brain Res Mol Brain Res* **35**: 31 40.

Taniguchi H, Tohyama A, Takagi T. (1996). Cloning and expression of a novel gene for a protein with leucine-rich repeats in the developing mouse nervous system. *Brain Res Mol Brain Res* **36**: 45 52.

Torres R, Schreiber-Agus N, Morgenbesser SD, DePinho RA. (1992). Myc and Max: a putative transcriptional complex in search of a cellular target. *Curr Opin Cell Biol* **4**: 468 474.

Truscott M, Denault JB, Goulet B, Leduy L, Salvesen GS, Nepveu A. (2007). Carboxy-terminal proteolytic processing of CUX1 by a caspase enables transcriptional activation in proliferating cells. *J Biol Chem* **282**: 30216 30226.

Wang J, Xie I, Allan S, Beach D, Hannon G. (1998). Myc activates telomerase. *Genes Dev* **12**: 1769 1774.

Weiss WA, Aldape K, Mohapatra G, Feuerstein BG, Bishop JM. (1997). Targeted expression of MYCN causes neuroblastoma in transgenic mice. *EMBO J* **16**: 2985 2995.

Supplementary Information accompanies the paper on the Oncogene website (http://www.nature.com/onc)

THE JOURNAL OF BIOLOGICAL CHEMISTRY VOL. 283, NO. 36, pp. 24426–24434, September 5, 2008

KIF1Bβ Functions as a Haploinsufficient Tumor Suppressor Gene Mapped to Chromosome 1p36.2 by Inducing Apoptotic Cell Death*[S]

Received for publication, March 25, 2008, and in revised form, June 9, 2008 Published, JBC Papers in Press, July 9, 2008, DOI 10.1074/jbc.M802316200

Arasambattu K. Munirajan[‡§¶], Kiyohiro Ando[‡], Akira Mukai[‡], Masato Takahashi[‡], Yusuke Suenaga[‡], Miki Ohira[‡], Tadayuki Koda[§], Toru Hirota[‖], Toshinori Ozaki[‡], and Akira Nakagawara[‡1]

From the [‡]Division of Biochemistry, Chiba Cancer Center Research Institute, Chiba 260-8717, Japan, [§]Research Center for Functional Genomics, Hisamitsu Pharmaceutical Company, Inc., Tokyo 141-8577, Japan, the [¶]Department of Genetics, Dr. ALM PG Institute of Basic Medical Sciences, University of Madras, 600-113 Chennai (Madras), India, and the [‖]Department of Experimental Pathology, The Cancer Institute, Tokyo 135-8550, Japan

Deletion of the distal region of chromosome 1 frequently occurs in a variety of human cancers, including aggressive neuroblastoma. Previously, we have identified a 500-kb homozygously deleted region at chromosome 1p36.2 harboring at least six genes in a neuroblastoma-derived cell line NB1/C201. Among them, only *KIF1Bβ*, a member of the kinesin superfamily proteins, induced apoptotic cell death. These results prompted us to address whether *KIF1Bβ* could be a tumor suppressor gene mapped to chromosome 1p36 in neuroblastoma. Hemizygous deletion of *KIF1Bβ* in primary neuroblastomas was significantly correlated with advanced stages ($p = 0.0013$) and *MYCN* amplification ($p < 0.001$), whereas the mutation rate of the *KIF1Bβ* gene was infrequent. Although *KIF1Bβ* allelic loss was significantly associated with a decrease in *KIF1Bβ* mRNA levels, its promoter region was not hypermethylated. Additionally, expression of *KIF1Bβ* was markedly down-regulated in advanced stages of tumors ($p < 0.001$). Enforced expression of *KIF1Bβ* resulted in an induction of apoptotic cell death in association with an increase in the number of cells entered into the G_2/M phase of the cell cycle, whereas its knockdown by either short interfering RNA or by a genetic suppressor element led to an accelerated cell proliferation or enhanced tumor formation in nude mice, respectively. Furthermore, we demonstrated that the rod region unique to *KIF1Bβ* is critical for the induction of apoptotic cell death in a p53-independent manner. Thus, *KIF1Bβ* may act as a haploinsufficient tumor suppressor, and its allelic loss may be involved in the pathogenesis of neuroblastoma and other cancers.

Neuroblastoma is one of the most common malignant solid tumors occurring in infancy and childhood and accounts for 10% of all pediatric cancers (1). Neuroblastomas are derived from sympathetic neuroblasts with various clinical outcomes from spontaneous regression because of neuronal differentiation and/or apoptotic cell death to malignant progression. Extensive cytogenetic and molecular genetic studies identified that genetic abnormalities such as loss of short arm of chromosome 1 (1p), amplification of *MYCN*, and 17q gain are frequently observed and often associated with poor clinical outcome (2, 3). The actual prevalence of 1p deletion in neuroblastoma is ~35% (4–9). The deleted regions were extensively mapped to identify the candidate tumor suppressor gene(s) that has been deleted out from this region (10–17). A chromosomal locus 1p36 is frequently deleted in aggressive neuroblastoma, pheochromocytoma, colon, liver, brain, breast, and other cancers (18, 19). Transfer of 1p chromosome segments into neuroblastoma-derived cell line NGP.1A.TR1 resulted in a significant suppression of their tumor formation (20). Furthermore, previous studies indicated that there is no single site of deletion on the distal part of 1p36, but there are at least three discrete regions that are commonly deleted in neuroblastoma, indicating that they may harbor potential tumor suppressor gene(s) (8).

Tumor suppressor genes, one of the main classes of cancer-associated genes, encode inhibitors of cell proliferation and/or activators of apoptotic cell death and are involved in a variety of molecular mechanisms behind cell growth suppression (21). Tumor suppressor genes frequently mutated in other malignancies do not appear to play a major role in the generation of neuroblastoma, indicating that development of this type of tumor employs one or more previously unidentified genetic pathways. To date, a majority of candidate tumor suppressor genes has been identified by mapping the minimal deleted region and searching for the intact homologous region of mutated genes. This experimental strategy fails when the second allele is silenced by promoter hypermethylation or the targeted gene is haploinsufficient for tumor suppression, a situation where loss of one allele confers a selective advantage for tumor growth. Several examples of such haploinsufficiency for tumor suppression have been demonstrated in the case of $p27^{KIP1}$, *p53*, and *PTEN* (22, 23).

We and other investigators have previously identified a 500-kb homozygous deletion at 1p36.2 harboring at least six

* This work was supported by the Ministry of Education, Culture, Sports, Science and Technology of Japan and the Ministry of Health, Labor and Welfare of Japan. The costs of publication of this article were defrayed in part by the payment of page charges. This article must therefore be hereby marked "*advertisement*" in accordance with 18 U.S.C. Section 1734 solely to indicate this fact.

[S] The on-line version of this article (available at http://www.jbc.org) contains supplemental Figs. S1–S5.

[1] To whom correspondence should be addressed: Division of Biochemistry, Chiba Cancer Center Research Institute, 666-2 Nitona, Chuo-ku, Chiba 260-8717, Japan. Tel.: 81-43-264-5431; Fax: 81-43-265-4459; E-mail: akiranak@chiba-cc.jp.

genes, *PEX14*, *UFD2a*, *KIF1B*, *CORT*, *DFF45*, and *PGD*, in a neuroblastoma-derived cell line NB1/C201 (12, 15, 24). In this study, we have demonstrated that only *KIF1Bβ*, a member of the kinesin 3 family genes (25), might be a tumor suppressor gene mapped to chromosome 1p36 in neuroblastoma. Kinesins are microtubule-dependent intracellular motors involved in the transport of organelles, vesicles, protein complexes, and RNA to specific destinations (26, 27). *KIF1B* encodes two alternatively spliced isoforms, including *KIF1Bα* and *KIF1Bβ*, and both form homodimers and transport mitochondria and synaptic vesicle precursors, respectively (28). The NH_2-terminal motor domain of *KIF1Bα* is identical to *KIF1Bβ*, whereas COOH-terminal tails share no structural homology. A point mutation in the ATP-binding site within the motor domain of *KIF1Bβ* has been closely linked to Charcot-Marie Tooth disease type 2A (29).

In this study, we cloned a full-length *KIF1Bβ* cDNA, generated recombinant adenovirus encoding *KIF1Bβ*, and examined its biological role in neuroblastoma and other cell lines. We systematically analyzed *KIF1Bβ* for LOH,[2] mutation, and promoter methylation. Our genetic and functional analyses clearly showed that *KIF1Bβ* is a tumor suppressor, although not a classic one. *KIF1Bβ* might act as a haploinsufficient tumor suppressor, and its down-regulation might potentially contribute to tumorigenesis of cancers, including neuroblastoma.

EXPERIMENTAL PROCEDURES

Cell Lines and Tumor Samples—Human neuroblastoma (NB) cell lines such as SH-SY5Y, NB1, and SK-N-BE were grown in RPMI 1640 medium supplemented with heat-inactivated fetal bovine serum, 100 units/ml penicillin, and 100 μg/ml streptomycin. NMuMG, COS7, HEK293, and HeLa cells were grown in Dulbecco's modified Eagle's medium containing 10% heat-inactivated fetal bovine serum, 100 units/ml penicillin, and 100 μg/ml streptomycin. Tumor DNA and RNA samples were obtained from our Neuroblastoma Resource Bank. Informed consent was obtained at each hospital.

GSE-mediated Tumor Formation in Nude Mice—GSE assay was performed as described previously (30). In brief, a cDNA fragment (nucleotide number 2658–3115 of GenBank™ accession number AB017133) corresponding to the unique region of *KIF1Bβ* was amplified by PCR-based strategy and subcloned into the HpaI site of the pLXSN vector in an antisense orientation to give pLXSN-antisense *KIF1Bβ*. NMuMG mammary gland cells (1×10^6 cells) infected with pLXSN or with pLXSN-antisense *KIF1Bβ* were inoculated subcutaneously into the femoral region of nude mice. In the experiments using live animals, we strictly followed the Chiba Cancer Center Research Institute guidelines and protocols for handling live animals.

Construction of Expression Plasmids and Recombinant Adenovirus—*KIF1Bβ* splicing variants I, III, and IV fused to the FLAG epitope at their NH_2 termini were amplified by PCR using cDNA prepared from CHP134 cells as a template and subcloned into pcDNA3.1 (Invitrogen). *KIF1Bβ-GFP* deletion constructs were produced by PCR-based amplification. The recombinant adenovirus was constructed as described previously (31). Briefly, *KIF1Bβ* cDNA was subcloned into pHMCMV6 adeno-shuttle vector. The shuttle vector was then digested with I-Ceu I and PI-Sce I and inserted into the identical restriction sites of the adenovirus expression vector pAdHM4. All of the recombinant vectors were verified by DNA sequencing. Recombinant adenoviruses were produced by transfecting the PacI-digested expression constructs into HEK293 cells. An expression vector encoding GFP was used to monitor the efficiency of infection.

Mutation Analysis—For the detection of *KIF1Bβ* mutations, we designed primer sets covering the motor domain and 2 kb of the 5′-upstream region of *KIF1Bβ*. After PCR-based amplification, PCR products were separated by 5% nondenaturing polyacrylamide gels. After electrophoresis, PCR products were gel-purified and subcloned into pGEM-T Easy Vector (Promega), and their DNA sequences were determined by an automated DNA sequencer (Applied Biosystems).

Flow Cytometry—Cells were fixed in ice-cold 70% ethanol, treated with 50 mM sodium citrate, 100 μg/ml RNase A, 50 μg/ml propidium iodide and subjected to FACS analysis (BD Biosciences) according to the manufacturer's instructions.

Construction of KIF1Bβ siRNA Expression Vector—An siRNA expression vector termed pMuniH1, in which the cytomegalovirus promoter of pcDNA 3.1 was replaced with the H1 promoter, was generated. Sense and antisense oligonucleotides for *KIF1Bβ* (nucleotide number 371–389 of GenBank™ accession number AB017183) were joined by a 9-base loop, annealed, and subcloned into pMuniH1.

Luciferase Reporter Assay—The genomic fragments corresponding nucleotide positions −887/+106, −630/+106, and −294/+106 of the *KIF1Bβ* gene were amplified from human placenta genomic DNA and cloned into pGL3-Basic luciferase reporter plasmid (Promega) to give pGL3(−887/+106), pGL3(−630/+106), and pGL3(−294/+106). For luciferase assay, SK-N-BE cells were transfected with pRL-TK (Promega) encoding *Renilla* luciferase cDNA and the indicated luciferase reporter constructs. Forty eight hours after transfection, firefly and *Renilla* luciferase activities were measured by dual-luciferase reporter assay system (Promega), and firefly luciferase activity was normalized to *Renilla* luciferase activity.

Methylation-specific PCR—The methylation status of the promoter region of *KIF1Bβ* was assessed by methylation-specific PCR as described previously (32).

Cell Cycle Analysis—Cells were fixed in 3.7% formaldehyde and permeabilized with 0.2% Triton X-100 and DNA was stained with 0.1 μg/ml of 4′,6′-diamidino-2-phenylindole. Cellular DNA content was analyzed by laser scanning cytometry (LSC2 System, Olympus).

Array-CGH Analysis—Array CGH analysis of 112 sporadic primary neuroblastomas using a chip carrying 2,464 bacterial artificial chromosome clones was conducted as described previously (33). All array-CGH data are available at NCBI Gene Expression Omnibus (GEO, www.ncbi.nlm.nih.gov) with accession number GSE 5784.

[2] The abbreviations used are: LOH, loss of heterogeneity; CGH, comparative genomic hybridization; FHA, forkhead-associated; GSE, genetic suppressor element; KIF, kinesin superfamily protein; NB, neuroblastoma; NGF, nerve growth factor; FACS, fluorescence-activated cell sorter; siRNA, short interfering RNA; MTT, 3-(4,5-dimethylthiazol-2-yl)-2,5-diphenyltetrazolium bromide; RT, reverse transcription; GFP, green fluorescent protein.

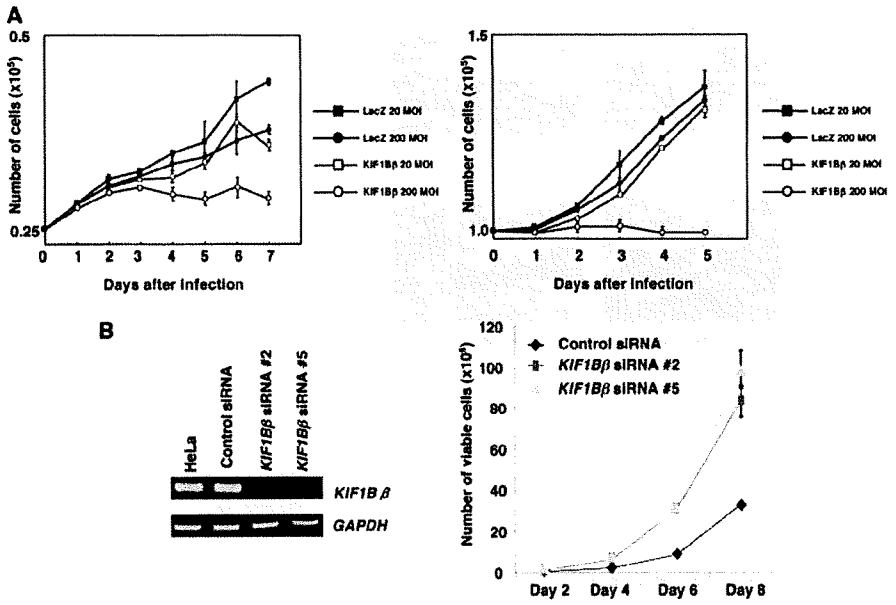

FIGURE 1. ***KIF1Bβ* has a growth-suppressive activity *in vitro*.** *A*, NB1 (*left panel*) and NMuMG (*right panel*) cells were infected with recombinant adenovirus encoding LacZ or *KIF1Bβ* at the indicated multiplicity of infection (*MOI*). At the indicated time points after infection, the number of viable cells was measured. *B*, HeLa cells stably expressing control siRNA-2 or siRNA-5 against *KIF1Bβ* were established, and the expression levels of the endogenous *KIF1Bβ* were examined by RT-PCR (*left panel*). Glyceraldehyde-3-phosphate dehydrogenase (*GAPDH*) was used as an internal control. Number of viable cells was measured at the indicated time points (*right panel*).

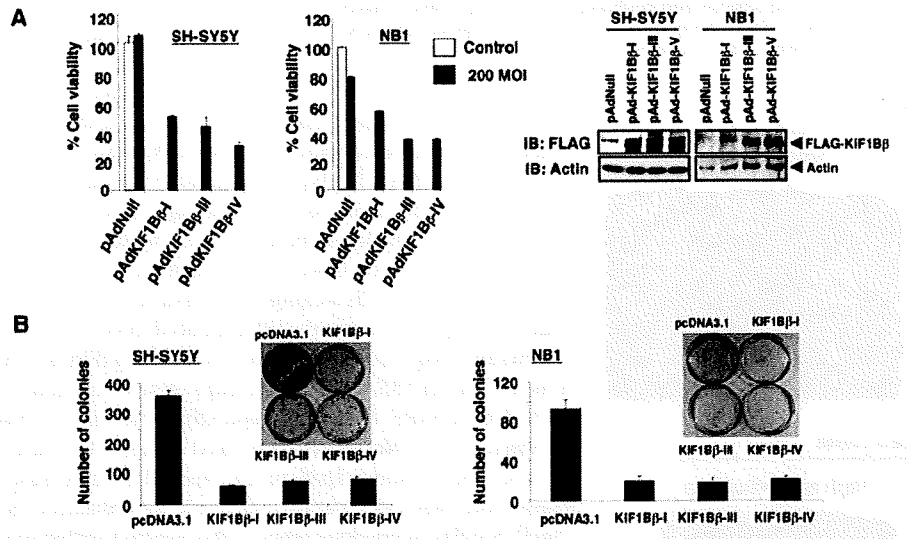

FIGURE 2. **Enforced expression of *KIF1Bβ* induces growth suppression in neuroblastoma-derived cell lines.** *A*, MTT assay. Neuroblastoma-derived SH-SY5Y and NB1 cells were infected with the indicated recombinant adenoviruses, including empty adenovirus (pAdNull) at a 200 multiplicity of infection (*MOI*) (*filled boxes*) or left untreated (*open boxes*). Twenty four hours after infection, infected SH-SY5Y and NB1 cells were seeded at a density of 1×10^3 cells/96-well plates and allowed to attach. Ninety six hours after infection, 10 μl of MTT solution was added to each well and incubated for 3 h at 37 °C (*left panel*). *Right panels* show the expression of the indicated splicing variants of KIF1Bβ as examined by immunoblotting (*IB*) with anti-FLAG antibody. *B*, colony formation assay. SH-SY5Y and NB1 cells were transfected with an empty plasmid or with the indicated expression plasmids. Forty eight hours after transfection, cells were transferred into fresh medium containing 500 μg/ml of G418 and incubated for 2 weeks. After selection with G418, G418-resistant viable colonies were stained with Giemsa solution, and number of colonies was scored.

Caspase Assay—Caspase activity was measured by using caspase-3/7 assay system (Promega) according to the manufacturer's instructions.

Statistics—The Student's *t* test was used as a statistical method. Statistical significance was declared if the *p* value was <0.05.

RESULTS

Identification of KIF1Bβ as a Candidate Tumor Suppressor Mapped to Chromosome 1p36.2—To search for a candidate tumor suppressor gene(s), we first transferred each of the above-mentioned six genes into NB1 and nontransformed NMuMG mouse epithelial cells (30), and we found that only *KIF1Bβ* induces growth suppression in a dose-dependent manner (Fig. 1*A*). In contrast, our preliminary observations indicated that its alternative splicing variant *KIF1Bα* lacking a COOH-terminal rod region has marginal effects on cell growth in NB1 cells (data not shown). In support of these results, siRNA-mediated knockdown of *KIF1Bβ* in HeLa cells without 1p loss markedly enhanced their cell growth (Fig. 1*B*). In addition, enforced expression of *KIF1Bβ* induced growth retardation in *p53*-deficient H1299 cells and HeLa cells in which p53 is inactivated because of the presence of E6-AP (data not shown).

Overexpression of KIF1Bβ in Neuroblastomas-induced Apoptotic Cell Death—During PCR-based screening of human *KIF1Bβ* cDNA from human neuroblastoma cell lines, we identified at least four splicing variants that lacked exons 14 and/or 15 (supplemental Fig. S1). Similar splicing variants have also been observed in mice and rats (34). We successfully generated recombinant adenoviruses for human KIF1Bβ-I, -III, and -IV variants (Fig. 2*A*). Enforced expression of these splicing variants promoted apoptotic cell death in both SH-SY5Y (without 1p loss) and NB1 neuroblastoma cell lines as determined by MTT and FACS analyses (Fig. 2*A* and supplemental Fig. S2). Consistent with these results, colony formation assay showed that all these KIF1Bβ splicing variants strongly reduced the number of drug-resistant colonies in SH-SY5Y and NB1 neuroblastoma cells (Fig. 2*B*). These findings suggest that multiple KIF1Bβ splicing isoforms

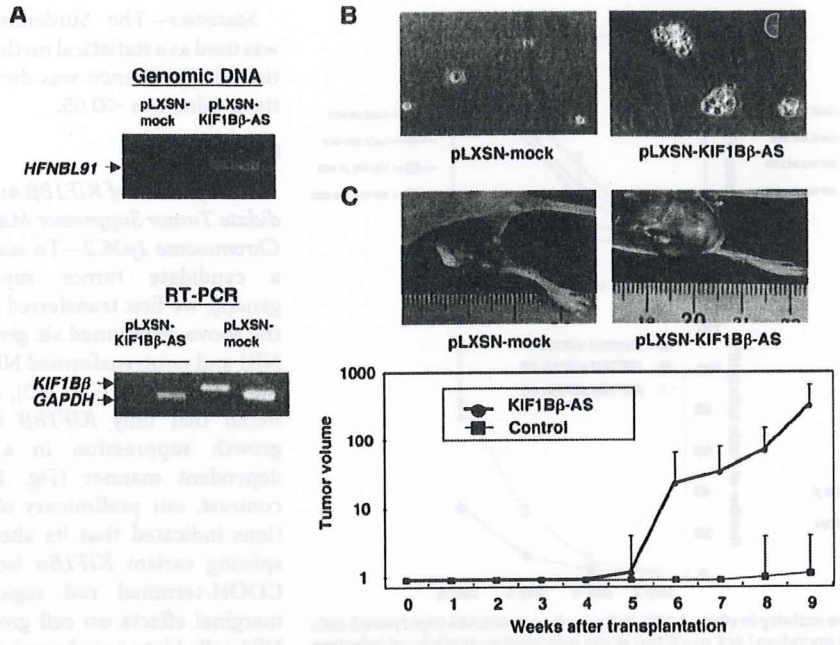

FIGURE 3. **Tumor formation *in vivo*.** *A*, NMuMG cells were infected with an empty retrovirus vector (pLXSN) or with pLXSN bearing mouse antisense *KIF1Bβ* (pLXSN-*KIF1Bβ*-AS). Genomic integration of the antisense *KIF1Bβ* was examined by PCR (*upper panel*). *Lower panel* shows the expression levels of *KIF1Bβ* as examined by RT-PCR. *Arrows* indicate the positions of PCR products corresponding to *KIF1Bβ* and *GAPDH*. *B*, NMuMG cells (5×10^4 cells) infected with pLXSN or pLXSN-KIF1Bβ-AS were suspended in 3 ml of 0.4% low melting agarose dissolved in culture medium, plated onto agarose bed consisting of 0.8% low-melting agarose, and incubated at 37 °C for 5 weeks. *C*, tumor formation in nude mice. NMuMG cells (1×10^6 cells) infected with the indicated retroviruses were injected subcutaneously and tumor volumes were estimated weekly (*lower panel*). *Upper panels* show tumors generated in nude mice.

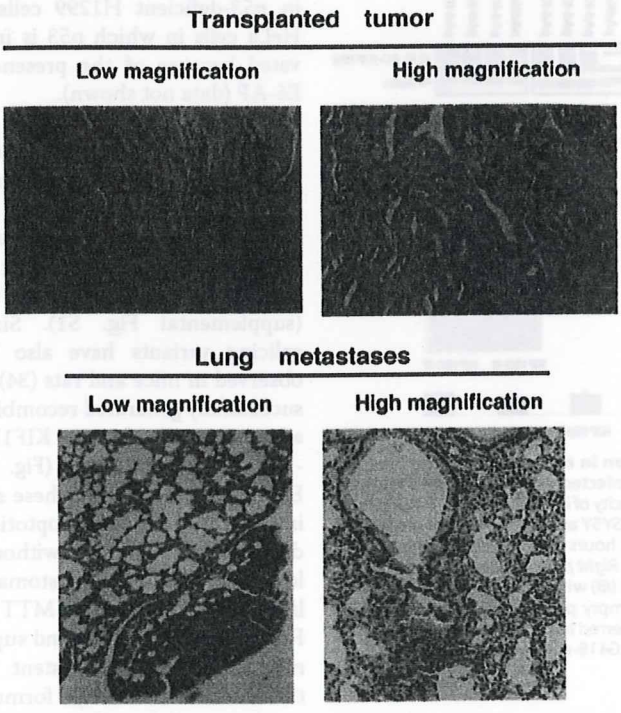

FIGURE 4. **Histology of tumors generated in nude mice.** Representative photographs of tumors (*upper panels*) and lung metastasis (*lower panels*) are shown. For histological analyses, tumor tissues were removed from animals and immediately fixed in 10% formaldehyde and embedded in paraffin, and 3-μm sections were stained with hematoxylin and eosin.

possess tumor suppressor activity. Intriguingly, the expression pattern of *KIF1Bβ* splicing variants was varied among various human tissues (supplemental Fig. S3).

Knockdown of KIF1Bβ Expression Accelerates Growth of NMuMG Cells and Tumor Formation in Nude Mice—We then asked whether genetic disruption of *KIF1Bβ* gene could be critical for tumorigenesis. For this purpose, we employed a genetic suppressor element (GSE) strategy (30). A mouse genomic DNA corresponding to a *KIF1Bβ* cDNA fragment (nucleotide number 2658–3115 of GenBank™ accession number AB017133) encoding the unique region of *KIF1Bβ* was subcloned into the retrovirus pLXSN vector in an antisense orientation to give pLXSN-KIF1Bβ-AS. NMuMG cells, immortalized mouse mammary gland cells, stably infected with pLXSN-KIF1Bβ-AS, showed more than 80% reduction in endogenous *KIF1Bβ* expression (Fig. 3*A*) and formed significantly larger colonies than empty vector-infected control cells in soft agar medium (Fig. 3*B*). In addition, all eight mice subcutaneously transplanted with NMuMG cells stably infected with pLXSN-KIF1Bβ-AS displayed remarkable tumor growth (Fig. 3*C*). On the other hand, only two of eight mice transplanted with the empty vector-infected cells formed tumors, which were smaller in both cases (note log scale in Fig. 3*C*). The tumors formed by cells lacking *KIF1Bβ* expression were histologically diagnosed as poorly differentiated invasive ductal carcinoma and frequently metastasized to the lung (Fig. 4). Thus, it is likely that KIF1Bβ exerts tumor-suppressive function *in vivo*.

LOH of KIF1Bβ Locus Is Frequently Observed in Primary Advanced Neuroblastomas—We next sought to search for LOH at chromosome 1p36 in 112 sporadic neuroblastomas using array-based comparative genomic hybridization (array-CGH). Similar to previous reports, the smallest region of overlap at the distal region of chromosome 1p identified in 37 primary neuroblastomas with 1p loss was between 1p36.22 and 1pter and included *KIF1B*, *CHD5*, *TP73*, and *SKI* (supplemental Fig. S4). Thirty two percent (30/95) of neuroblastomas examined had lost one *KIF1Bβ* allele as determined by quantitative real time genomic PCR (Table 1). *KIF1Bβ* was hemizygously deleted in 18% of early neuroblastomas (stages 1 and 2, $n = 51$), in 55% of advanced neuroblastomas (stages 3 and 4, $n = 38$) ($p = 0.0013$), in 13% of primary neuroblastomas with a single copy of *MYCN* ($n = 70$), and in 84% of *MYCN*-amplified primary neuroblastomas ($n = 25$) ($p < 0.001$). No homozygous deletion was detected in the primary tumors examined.

Decreased Expression of KIF1Bβ Is Associated with Monoallelic Loss of the Gene in Primary Neuroblastomas—We examined expression levels of *KIF1Bβ* mRNA in 102 primary neuroblastomas by using both semi-quantitative and quantitative real time PCRs. As shown in Fig. 5, *A* and *B*, expression levels of *KIF1Bβ* mRNA were significantly higher in tumors at favorable stages (1, 2, and 4s, 1.654 ± 0.257, mean ± S.E., $n = 60$) than in those at advanced stages (3 and 4, 0.503 ± 0.180, $n = 42$, $p < 0.001$). To address whether its expression levels could be correlated with number of alleles at the *KIF1Bβ* gene locus, we examined primary tumors with a diploid karyotype. As shown in the *lower panel* of Fig. 5*B*, tumors with monoallelic loss of *KIF1Bβ* gene locus expressed significantly lower levels of *KIF1Bβ* mRNA (0.126 ± 0.092, $n = 13$) as compared with those with two *KIF1Bβ* alleles (0.364 ± 0.035, $n = 16$, $p = 0.019$). These results suggest that *KIF1Bβ* is a haploinsufficient tumor suppressor gene in high risk neuroblastomas.

TABLE 1
Frequency of LOH of the *KIF1B* gene
LOH was examined by both array-CGH and quantitative real time PCR using genomic DNA obtained from primary neuroblastomas (tumor cells component, >70%). The cutoff value of the LOH score was 0.8 in the latter.

Category	*n*	*KIF1B* LOH	
		LOH (+)	%
Stage			
1	36	6	17
2	15	3	20
3	7	3	43
4	31	18	58
4s	6	0	0
MYCN			
Single copy	70	9	13
Amplification	25	21	84
Total	95	30	32

No Promoter Methylation and Rare Mutations Are Observed in Neuroblastoma Cell Lines and Primary Neuroblastomas—Our initial mutation searches of *KIF1Bβ* gene were focused on its motor domain and the proximal (~2 kb) promoter region in 21 primary neuroblastomas with 1p36 LOH and in 17 neuroblastoma cell lines. As shown in Table 2, we identified only a silent mutation GCC-GCG (at codon 95) in two primary tumors, a 2-bp (CC) deletion (at −113/−114) and G-A base change (at −336) in the *KIF1Bβ* promoter region in three primary tumors and four neuroblastoma cell lines. Because these aberrations were also found in the control samples, it is likely that these base changes reflect single nucleotide polymorphisms of the Japanese population.

To further extend our mutation searches, we have examined the presence or absence of *KIF1Bβ* mutations within its whole coding region in 100 primary neuroblastoma tissues. Finally, we found out the missense mutations (N737S) in six independent cases. However, their functional significances remained unclear.

Methylation of CpG islands in the promoters has been considered to be another well recognized molecular mechanism behind the inactivation of the tumor suppressor gene. To determine whether the methylation of CpG island could contribute to the inactivation of *KIF1Bβ*, the region spanning exon 1 and 5′-upstream sequences (nucleotide number −877 to +106) of *KIF1Bβ* was cloned and analyzed for promoter activity by luciferase reporter assay. As shown in Fig. 6, *A* and *B*, *KIF1Bβ* promoter region existed at nucleotide position between −630 and −294. We then identified *KIF1Bβ* CpG islands within the promoter region and investigated whether these CpGs could be methylated in primary neuroblastomas as well as cell lines. The methylation-specific PCR analysis demonstrated that all of the CpG clusters are unmethylated, suggesting that *KIF1Bβ* is not inactivated by methylation (Fig. 6*C*).

The COOH-terminal Region between FHA and Pleckstrin Homology Domains of KIF1Bβ Is Responsible to Induce Apoptotic Cell Death—To map a critical domain(s) of KIF1Bβ responsible for its tumor-suppressive function, we generated NH_2-

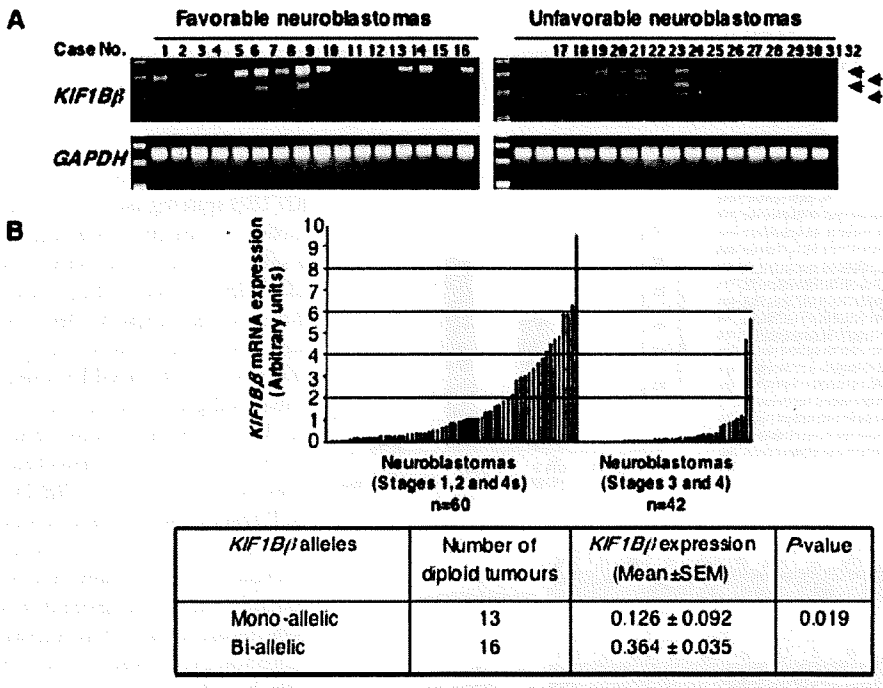

KIF1Bβ alleles	Number of diploid tumours	*KIF1Bβ* expression (Mean±SEM)	*P* value
Mono-allelic	13	0.126 ± 0.092	0.019
Bi-allelic	16	0.364 ± 0.035	

FIGURE 5. **Expression levels of *KIF1Bβ* in primary neuroblastomas.** *A*, semi-quantitative RT-PCR analysis. Total RNA was prepared from favorable ($n = 16$; stages 1 and 2, *MYCN* single copy) and unfavorable ($n = 16$; stages 3 and 4, *MYCN* amplified) neuroblastomas and subjected to semi-quantitative RT-PCR to examine the expression levels of *KIF1Bβ*. Glyceraldehyde-3-phosphate dehydrogenase (*GAPDH*) was used as an internal control. *B*, quantitative real time PCR. Expression levels of *KIF1Bβ* were standardized using the corresponding glyceraldehyde-3-phosphate dehydrogenase value of each neuroblastoma sample. The relative expression levels of *KIF1Bβ* in favorable (stages 1, 2,and 4s) and advanced (stages 3 and 4) neuroblastomas are shown (*upper panel*). *Lower panel* shows a significant correlation between mono-allelic loss of *KIF1Bβ* gene and its lower expression levels.

TABLE 2
Mutation analyses of *KIF1Bβ* gene

S. no.	Case no.	Exon 4–6	KIF exon 15	KIF promotor F12	KIF promotor F11	F/UF[a]
1	NB-1					NA
2	NB-2		G→A	Δ2 bp (−113–4)	G→A (−366)	NA
3	NB-3					UF
4	NB-4		G→A			UF
5	NB-5		/			NA
6	NB-6	GCC/GCG (95)	/	Δ2 bp (−113–4)	G→A (−366)	F
7	NB-7		/			UF
8	NB-8		/			UF
9	NB-9		/			F
10	NB-10		/			F
11	NB-11		/			UF
12	NB-12		/			UF
13	NB-13	GCC/GCG (95)	/	Δ2 bp (−113–4)	G→A (−366)	UF
14	NB-14		/			NA
15	NB-15		/			NA
16	NB-16		/			NA
17	NB-17		/			NA
18	NB-18		/			NA
19	NB-19		/			UF
20	NB-20		/			NA
21	NB-21		/			F
22	NB-GAMB		G>A	Δ2 bp (−113–4)	G→A (−366)	Cell line
23	NB-GOTO/P3					Cell line
24	NB-KAN		G>A	Δ2 bp (−113–4)	G→A (−366)	Cell line
25	NB-LHN		G>A	Δ2 bp (−113–4)	G→A (−366)	Cell line
26	NB-NB9					Cell line
27	NB-NB69		/			Cell line
28	NB-NBLS		/			Cell line
29	NB-NBTu-1		/			Cell line
30	NB-NLF		/			Cell line
31	NB-NMB		/	Δ2 bp (−113–4)	G→A (−366)	Cell line
32	NB-OAN		/			Cell line
33	NB-SK-N-AS		/			Cell line
34	NB-SK-N-BE		/			Cell line
35	NB-SK-N-SH		/			Cell line
36	NB-SH-SY5Y		/			Cell line
37	NB-CHP134		/			Cell line
38	NB-TGW	GCC/GCG (95)	/			Cell line

[a] For Shimada classification, F indicates favorable histology; UF indicates unfavorable histology, and NA indicates not analyzed.

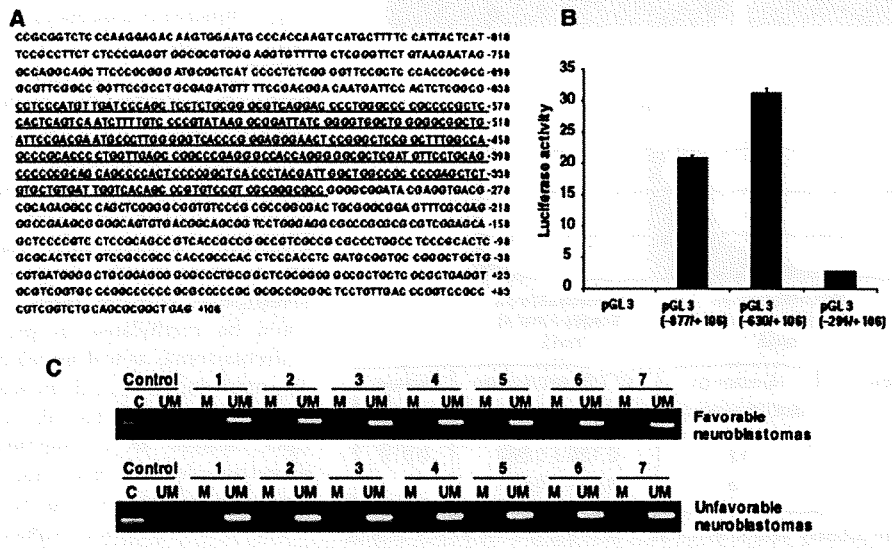

FIGURE 6. **Identification of the promoter region of human *KIF1Bβ* gene and its methylation status.** *A*, nucleotide sequence of 5′-upstream region and a part of exon 1 of human *KIF1Bβ* gene. +1 indicates the first nucleotide of exon 1. CpG island is indicated by *underline*. *B*, luciferase reporter assay. Neuroblastoma-derived SK-N-BE cells were transiently co-transfected with the constant amount of pRL-TK encoding *Renilla* luciferase cDNA and the indicated luciferase reporter constructs. Forty eight hours after transfection, cells were lysed, and their luciferase activities were measured. *C*, methylation-specific PCR. Methylation status of the promoter region of *KIF1Bβ* gene in primary neuroblastomas was examined by methylation-specific PCR. *M*, methylated; *UM*, unmethylated; *C*, control.

terminal deletion mutants of KIF1Bβ splicing isoform IV lacking motor domain (KIF1Bβ-IV-Del 1-GFP), motor and FHA domains (KIF1Bβ-IV-Del 2-GFP), coiled-coil domain (KIF1Bβ-IV-Del 3-GFP), and FHA and coiled-coil domains (KIF1Bβ-IV-Del 4-GFP) fused with enhanced green fluorescent protein at their COOH termini (Fig. 7*A*). COS7 cells were transfected with wild-type or with KIF1Bβ-IV-Del-GFP fusion constructs and followed by live confocal laser scanning microscopy. Forty eight hours after transfection, KIF1Bβ-GFP-positive cells began to lose their normal cell morphology. Seventy two hours after transfection, most of the cells underwent apoptotic cell death and detached from the cell culture dish (Fig. 7, *B* and *D*). Expression of splicing variants-I, -III, and -IV along with deletion mutants of splicing variant-IV lacking the motor

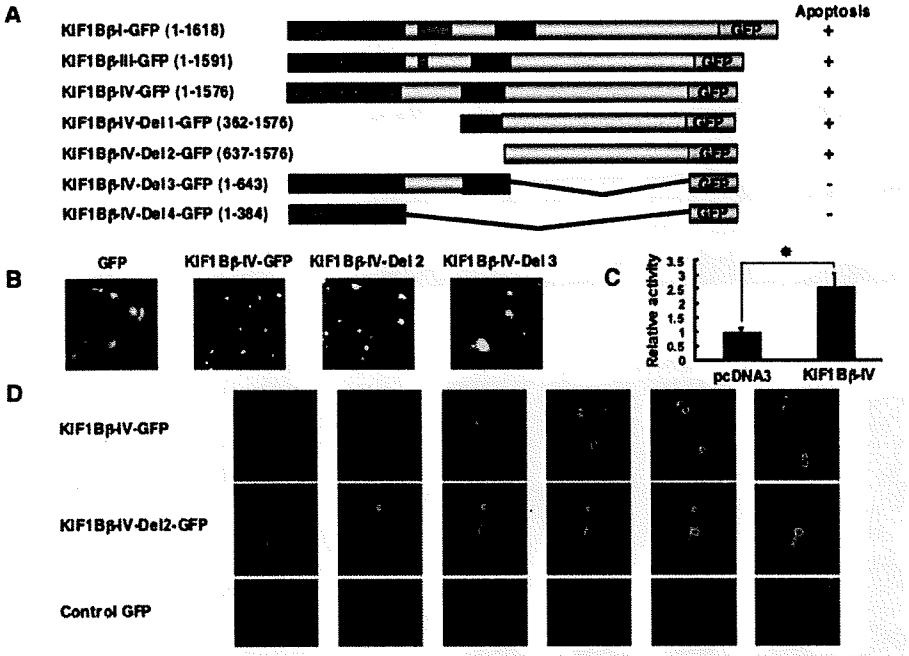

FIGURE 7. **The coiled-coil region is required for *KIF1Bβ*-mediated apoptotic cell death.** *A*, schematic representation of GFP-tagged KIF1Bβ deletion mutants and summary of their ability to induce apoptotic cell death. *B*, COS7 cells were transiently transfected with the indicated expression plasmids. Forty eight hours after transfection, morphologies of GFP-positive cells were examined by a confocal laser scanning microscope. *C*, caspase activity. HeLa cells were transiently transfected with the indicated expression plasmids. Forty eight hours after transfection, cell lysates were prepared, and their caspase activities were measured. Statistically significant differences are indicated by *asterisks* ($p < 0.05$). *D*, time course experiments. The indicated expression plasmids were transiently introduced into COS7 cells. Forty eight hours after transfection, changes of morphology of GFP-positive cells were monitored for 12 h.

domain (with or without FHA domain) also induced apoptotic cell death. In contrast, expression of KIF1Bβ mutants lacking the COOH-terminal rod domain did not promote apoptotic cell death (Fig. 7, *A* and *B*). Under our experimental conditions, enforced expression of KIF1Bβ variant-IV resulted in a significant increase in the caspase activities (Fig. 7*C*), suggesting that KIF1Bβ-mediated apoptotic cell death might be regulated in a caspase-dependent manner. Our further analysis using other deletion mutants revealed that the 807 amino acids death-inducing region is located between FHA and pleckstrin homology domains (data not shown).

To determine whether the kinesin activity of KIF1Bβ could be necessary for its tumor-suppressive function, we introduced a Q98L mutation within a consensus ATP-binding site of KIF1Bβ-IV splicing variant (Fig. 8*A*). This mutation disrupts the motor function of KIF1Bβ (29). In addition, a KIF1Bβ-IV splicing variant carrying two point mutations (Q560A and D568A) within its highly conserved amino acid residues of FHA domain, which may be critical for binding to Ser/Thr-phosphorylated motifs of the interacting proteins, was also generated. In addition to these two mutants, we also generated an additional mutant bearing Q98L, Q560A, and D568A. These three mutants, however, retained an ability to induce apoptotic cell death, suggesting that KIF1Bβ-mediated apoptotic cell death does not require its ability to transport cargo using its motor domain (Fig. 8*B*).

DISCUSSION

In this study, we have shown that the *KIF1Bβ* gene is hemizygously deleted especially in aggressive primary neuroblastoma tumors, and its mutation is infrequent. The expression of *KIF1Bβ* was kept at quite a low level in aggressive neuroblastoma subsets, even though no methylation of its promoter region was observed. One of the well known haploinsufficient tumor suppressors is the cyclin-dependent kinase inhibitor $p27^{KIP1}$ (35). The heterozygous mice of $p27^{KIP1}$ developed tumors when mice were treated with tumor-promoting agents, and tumors retained the normal $p27^{KIP1}$ allele. Additionally, hemizygous loss of $p27^{KIP1}$ and/or reduced expression level of $p27^{KIP1}$ conferred poor prognosis in human cancers (36). Taken together, our present results suggest that, like $p27^{KIP1}$, *KIF1Bβ* is a haploinsufficient tumor suppressor gene of neuroblastoma, and its function to induce apoptotic cell death is regulated in a p53-independent manner. Although homozygous deletion or mutations of *KIF1Bβ* were rarely detectable in this study, several losses of function mutations in the coding region of *KIF1Bβ* gene in a large number of primary neuroblastomas, pheochromocytomas, and medulloblastomas have now been identified.[3] Homozygous deletion of *KIF1B* in mice resulted in death just after birth because of apnea. However, heterozygous mice are viable with a phenotype resembling Charcot-Marie-Tooth disease type 2A (29). To date, no information has been available in the literature regarding spontaneous tumor formation in *KIF1B*-heterozygous mice. It is possible that these mice have not been followed long enough or that loss of one *KIF1B* allele is not sufficient for tumor formation and requires cooperating mutations for spontaneous tumor formation. Since there is functional disruption of wild-type p53 because of its mislocalization, haploinsufficiency of the *KIF1Bβ* gene might contribute to tumorigenesis of aggressive neuroblastomas with 1p LOH and *MYCN* amplification (37). *KIF1Bβ* might also be involved in tumorigenesis in combination with other contiguous 1p36.3 genes such as *p73* (38) and *CHD5* (39).

Finally, we have identified four different splicing variants of KIF1Bβ. However, colony formation assay revealed that all of the splicing variants almost equally suppress cell growth, indicating that its tumor-suppressive function may not be dependent on alternative splicing events. The deletion construct termed Del 2-GFP encoding amino acid residues 637–1576

[3] S. Schlisio and W. G. Kaelin, Jr., personal communication.

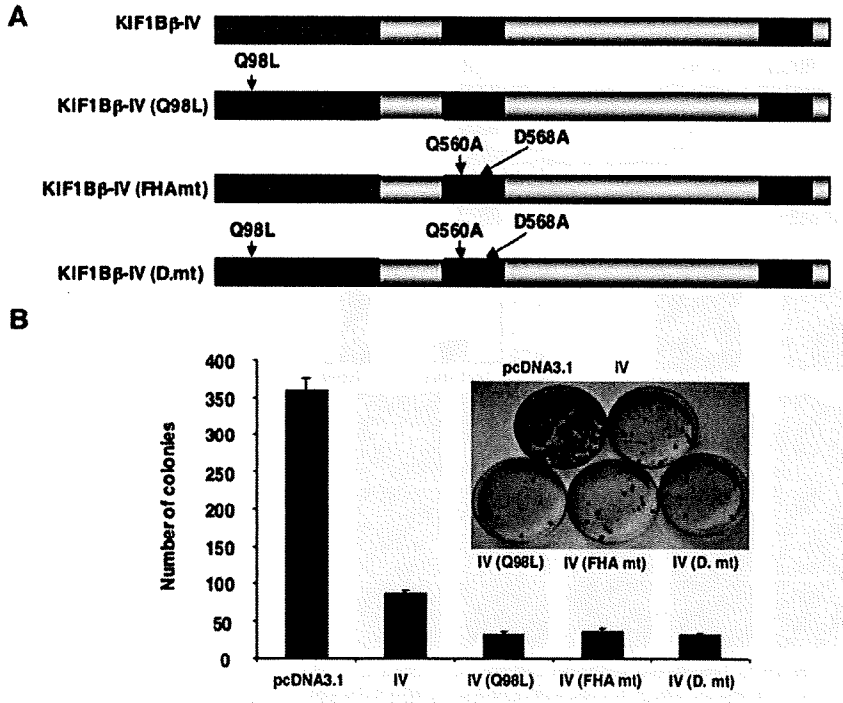

FIGURE 8. **Motor and FHA domains are not required for *KIF1Bβ*-mediated growth suppression.** *A*, schematic drawing of mutant forms of KIF1Bβ. Point mutations (Q98L, Q560A, and D568A) were introduced into *KIF1Bβ* by using the QuickChange XL site-directed mutagenesis kit (Stratagene) following the manufacturer's recommendations. *B*, colony formation assay. SH-SY5Y cells were transfected with an empty vector or with the indicated expression vectors. Forty eight hours after transfection, cells were transferred into fresh medium containing 500 μg/ml of G418. Two weeks after selection, G418-resistant colonies were fixed and stained with Giemsa solution, and number of drug-resistant colonies was scored.

induced apoptotic cell death similar to wild-type KIF1Bβ. Therefore, this region containing two predicted coiled-coils (amino acid residues 668–737 and 841–863) alone is sufficient for pro-apoptotic function of KIF1Bβ. The coiled-coil motifs are amphipathic oligomerization motifs. The tumor suppressor par-4 with a potential coiled-coil structure induced apoptotic cell death in prostate cancer cell lines (40, 41). Moreover, a putative coiled-coil domain of potential tumor suppressor protein, Prohibitin, has been shown to be sufficient to repress E2F1-mediated transcription and induction of apoptotic cell death (42).

In neuroblastoma, polyploidy is very common, which is often associated with a better prognosis. The precise molecular mechanisms underlying this phenomenon still remain unclear. Recently, defects in mitotic spindle check point gene products such as MAD1, MAD2, BUB1, BUB3, and BUBR1 have been implicated in the generation of polyploidy (43). Intriguingly, attached cells expressing GFP-tagged KIF1Bβ splicing variants exhibited a perturbation of G_2/M progression and multinucleation (supplemental Fig. S5). The precise molecular mechanisms by which KIF1Bβ could promote these cellular abnormalities and apoptotic cell death are currently unknown. On the other hand, down-regulation of KIF1Bβ resulted in augmented cell proliferation *in vitro* and tumor formation *in vivo*, indicating that KIF1Bβ might have a critical role in the regulation of mitosis like other mitotic kinesins (44). It is conceivable that KIF1Bβ might act in a dominant inhibitory manner to sequester fundamental cytoplasmic factors that are required for proper cell cycle progression. In this connection, we are undertaking to identify the KIF1Bβ-binding partner(s), which might clarify the molecular mechanisms behind growth suppression and/or apoptotic cell death mediated by KIF1Bβ.

The nerve growth factor (NGF) dependence of tumor cells through the TrkA-$p75^{NTR}$ receptor complex plays a critical role in the regulation of the spontaneous regression and differentiation in neuroblastoma (45). NGF depletion-induced apoptotic cell death is blocked in aggressive neuroblastoma (46). The findings showing that expression of *KIF1Bβ* also increases during apoptotic cell death triggered by NGF depletion in PC12 cells[3] strengthen the significance of the tumor suppressor function of KIF1Bβ in primary neuroblastomas and pheochromocytoma. Indeed, some kinesin family proteins are involved in the regulation of apoptotic cell death in developing neurons (47). In conclusion, our present results unveiled that *KIF1Bβ*, mapped to chromosome 1p36.2, is the candidate tumor suppressor gene of the kinesin family functioning in a manner of haploinsufficiency.

Acknowledgments—We thank Hajime Kageyama for help in FACS analysis and DNA sequencing; Yuki Nakamura, Natsue Kitabayashi, and Ayaka Nobusato for their excellent technical assistance; Drs. Keizo Takenaga, Kou Miyazaki, Hisashi Tokita, Nobumoto Tomioka, Yoko Nakamura, and Daihachiro Tomotsune for helpful discussions; and Drs. E. Thavathiru and Margaret Das for critical reading of the manuscript.

REFERENCES

1. Westemann, F., and Schwab, M. (2002) *Cancer Lett.* **184,** 127–147
2. Brodeur, G. M., Seeger, R. C., Schwab, M., Varmus, H. E., and Bishop, J. M. (1984) *Science* **224,** 1121–1124
3. Caron, H. (1995) *Med. Pediatr. Oncol.* **24,** 215–221
4. Gehring, M., Berthold, R., Edler, L., Schwab, M., and Amler, L. C. (1995) *Cancer Res.* **55,** 5366–5369
5. White, P. S., Maris, J. M., Beltinger, C., Sulman, E., Marshall, H. N., Fujimori, M., Kaufman, B. A., Biegel, J. A., Allen, C., Hilliard, C., Valentine, M. B., Look, A. T., Enomoto, H., Sakiyama, S., and Brodeur, G. M. (1995) *Proc. Natl. Acad. Sci. U. S. A.* **92,** 5520–5524
6. Martinsson, T., Sjoberg, R. M., Hedborg, F., and Kongner, P. (1995) *Cancer Res.* **55,** 5681–5686
7. White, P. S., Thompson, P. M., Seifried, B. A., Sulman, E. P., Jensen, S. J., Guo, C., Maris, J. M., Hogarty, M. D., Allen, C., Biegel, J. A., Matise, T. C., Gregory, S. G., Reynolds, C. P., and Brodeur, G. M. (2001) *Med. Pediatr. Oncol.* **36,** 37–41

8. Brodeur, G. M. (2003) *Nat. Rev. Cancer* **3,** 203–216
9. White, P. S., Thompson, P. M., Gotoh, T., Okawa, E. R., Igarashi, J., Kok, M., Winter, C., Gregory, S. G., Hogarty, M. D., Maris, J. M., and Brodeur, G. M. (2005) *Oncogene* **24,** 2684–2694
10. Hogarty, M. D., Liu, X., Guo, C., Thompson, P. M., Weiss, M. J., White, P. S., Sulman, E. P., Brodeur, G. M., and Maris, J. M. (2000) *Med. Pediatr. Oncol.* **6,** 512–515
11. Nakagawara, A., Ohira, M., Kageyama, H., Mihara, M., Furuta, S., Machida, T., Takayasu, H., Islam, A., Nakamura, Y., Takahashi, M., Shishikura, T., Kaneko, Y., Toyoda, A., Hattori, M., Sakaki, Y., Ohki, M., Horii, A., Soeda, E., Inazawa, J., Seki, N., Kuma, H., Nozawa, I., and Sakiyama, S. (2000) *Med. Pediatr. Oncol.* **35,** 516–521
12. Ohira, M., Kageyama, H., Mihara, M., Furuta, S., Machida, T., Shishikura, T., Takayasu, H., Islam, A., Nakamura, Y., Takahashi, M., Tomioka, N., Sakiyama, S., Kaneko, Y., Toyoda, A., Hattori, M., Sakaki, Y., Ohki, M., Horii, A., Soeda, E., Inazawa, J., Seki, N., Kuma, H., Nozawa, I., and Nakagawara, A. (2000) *Oncogene* **19,** 4302–4307
13. Bauer, A., Savelveva, L., Claas, A., Praml, C., Berthold, F., and Schwab, M. (2001) *Genes Chromosomes Cancer* **31,** 228–239
14. Caron, H., Spieker, N., Godfried, M., Veenstra, M., van Sluis, P., de Kraker, J., Voûte, P., and Versteeg, R. (2001) *Genes Chromosomes Cancer* **30,** 168–174
15. Chen, Y. Z., Soeda, E., Yang, H. W., Takita, J., Chai, L., Horii, A., Inazawa, J., Ohki, M., and Hayashi, Y. (2001) *Genes Chromosomes Cancer* **31,** 326–332
16. Ejeskar, K., Sjoberg, R. M., Abel, F., Kogner, P., Ambros, P. F., and Martinsson, T. (2001) *Med. Pediatr. Oncol.* **36,** 61–66
17. Mosse, Y. P., Greshock, J., Margolin, A., Naylor, T., Cole, K., Khazi, D., Hii, G., Winter, C., Shahzad, S., Asziz, M. U., Biegel, J. A., Weber, B. L., and Maris, J. M. (2005) *Genes Chromosomes Cancer* **43,** 390–403
18. Schwab, M., Praml, C., and Amler, L. C. (1996) *Genes Chromosomes Cancer* **16,** 211–229
19. Schwab, M., Westermann, F., Hero, B., and Berthold, F. (2003) *Lancet* **4,** 472–480
20. Bader, S. A., Fasching, C., Brodeur, G. M., and Stanbridge, E. J. (1991) *Cell Growth & Differ.* **5,** 245–255
21. Sherr, C. J. (2004) *Cell* **116,** 235–246
22. Cook, W. D., and McCaw, B. J. (2000) *Oncogene* **19,** 3434–3438
23. Fodde, R., and Smits, R. (2002) *Science* **298,** 761–763
24. Nagai, M., Ichimiya, S., Ozaki, T., Seki, N., Mihara, M., Furuta, S., Ohira, M., Tomioka, N., Nomura, N., Sakiyama, S., Kubo, O., Takakura, K., Hori, T., and Nakagawara, A. (2000) *Int. J. Oncol.* **16,** 907–916
25. Lawrence, C. J., Dawe, R. K., Christie, K. R., Cleveland, D. W., Dawson, S. C., Endow, S. A., Goldstein, L. S., Goodson, H. V., Hirokawa, N., Howard, J., Malmberg, R. L., McIntosh, J. R., Miki, H., Mitchison, T. J., Okada, Y., Reddy, A. S., Saxton, W. M., Schliwa, M., Scholey, J. M., Vale, R. D., Walczak, C. E., and Wordeman, L. (2004) *J. Cell Biol.* **167,** 19–22
26. Hirokawa, N. (1998) *Science* **279,** 519–526
27. Goldstein, L. S., and Philp, A. V. (1999) *Annu. Rev. Cell Dev. Biol.* **15,** 141–183
28. Nangaku, M., Sato-Yoshitake, R., Okada, Y., Noda, Y., Takemura, R., Yamazaki, H., and Hirokawa, N. (1994) *Cell* **79,** 1209–1220
29. Zhao, C., Takita, J., Tanaka, Y., Setou, M., Nakagawa, T., Takeda, S., Yang, H. W., Terada, S., Nakata, T., Takei, Y., Saito, M., Tsuji, S., Hayashi, Y., and Hirokawa, N. (2001) *Cell* **105,** 587–597
30. Garkavtsev, I., Kazarov, A., Gudkov, A., and Riabowol, K. (1996) *Nat. Genet.* **14,** 415–420
31. Mizuguchi, H., and Kay, M. A. (1998) *Hum. Gene Ther.* **9,** 2577–2583
32. Herman, J. G., Graff, J. R., Myohansen, S., Nelkin, B. D., and Baylin, S. B. (1996) *Proc. Natl. Acad. Sci. U. S. A.* **93,** 9821–9826
33. Tomioka, N., Oba, S., Ohira, M., Misra, A., Fridlyand, J., Ishii, S., Nakamura, Y., Isogai, E., Hirata, T., Yoshida, Y., Todo, S., Kaneko, Y., Albertson, D. G., Pinkel, D., Feuerstein, B. G., and Nakagawara, A. (2008) *Oncogene* **27,** 441–449
34. Gong, T. W., Winnicki, R. S., Kohrman, D. C., and Lomax, M. I. (1999) *Gene (Amst.)* **239,** 117–127
35. Fero, M. L., Randel, E., Gurley, K. E., Roberts, J. M., and Kemp, C. J. (1998) *Nature* **396,** 177–180
36. Blain, S. W., Scher, H. I., Cordon-Cardo, C., and Koff, A. (2003) *Cancer Cell* **3,** 111–115
37. Moll, U. M., LaQuaglia, M., Benard, J., and Riou, G. (1995) *Proc. Natl. Acad. Sci. U. S. A.* **92,** 4407–4411
38. Ichimiya, S., Nimura, Y., Kageyama, H., Takada, N., Sunahara, M., Shishikura, T., Nakamura, Y., Sakiyama, S., Seki, N., Ohira, M., Kaneko, Y., McKeon, F., Caput, D., and Nakagawara, A. (2001) *Med. Pediatr. Oncol.* **36,** 42–44
39. Bagchi, A., Papazoglu, C., Wu, Y., Capurso, D., Brodt, M., Francis, D., Bredel, M., Vogel, H., and Mills, A. A. (2007) *Cell* **128,** 459–475
40. Sells, S. F., Han, S. S., Muthukkumar, S., Maddiwar, N., Johnstone, R., Boghaert, E., Gillis, D., Liu, G., Nair, P., Monnig, S., Collini, P., Mattson, M. P., Sukhatme, V. P., Zimmer, S. G., Wood, D. P., Jr., McRoberts, J. W., Shi, Y., and Rangnekar, V. M. (1997) *Mol. Cell. Biol.* **17,** 3823–3832
41. Dutta, K., Engler, F. A., Cotton, L., Alexandrov, A., Bedi, G. S., Colquhoun, J., and Pascal, S. M. (2003) *Protein Sci.* **12,** 257–265
42. Joshi, B., Ko, D., Ordonez-Ercan, D., and Chellappan, D. (2003) *Biochem. Biophys. Res. Commun.* **312,** 459–466
43. Bharadwaj, R., and Yu, H. (2004) *Oncogene* **23,** 2016–2027
44. Endow, S. A. (1999) *Eur. J. Biochem.* **262,** 12–18
45. Nakagawara, A. (1998) *Med. Pediatr. Oncol.* **31,** 113–115
46. Nakagawara, A., Arima-Nakagawara, M., Scavarda, N. J., Azar, C. G., Cantor, A. B., and Brodeur, G. M. (1993) *N. Engl. J. Med.* **328,** 847–854
47. Midorikawa, R., Takei, Y., and Hirokawa, N. (2006) *Cell* **125,** 371–383

Vol 455|16 October 2008|doi:10.1038/nature07399

nature

LETTERS

Oncogenic mutations of ALK kinase in neuroblastoma

Yuyan Chen[1,2,3]*, Junko Takita[1,2,3]*, Young Lim Choi[4]*, Motohiro Kato[1,3], Miki Ohira[5], Masashi Sanada[2,3,6], Lili Wang[2,3,6], Manabu Soda[4], Akira Kikuchi[7], Takashi Igarashi[1], Akira Nakagawara[5], Yasuhide Hayashi[8], Hiroyuki Mano[4,6] & Seishi Ogawa[2,3,6]

Neuroblastoma in advanced stages is one of the most intractable paediatric cancers, even with recent therapeutic advances[1]. Neuroblastoma harbours a variety of genetic changes, including a high frequency of *MYCN* amplification, loss of heterozygosity at 1p36 and 11q, and gain of genetic material from 17q, all of which have been implicated in the pathogenesis of neuroblastoma[2–5]. However, the scarcity of reliable molecular targets has hampered the development of effective therapeutic agents targeting neuroblastoma. Here we show that the anaplastic lymphoma kinase (ALK), originally identified as a fusion kinase in a subtype of non-Hodgkin's lymphoma (NPM–ALK)[6–8] and more recently in adenocarcinoma of lung (EML4–ALK)[9,10], is also a frequent target of genetic alteration in advanced neuroblastoma. According to our genome-wide scans of genetic lesions in 215 primary neuroblastoma samples using high-density single-nucleotide polymorphism genotyping microarrays[11–14], the *ALK* locus, centromeric to the *MYCN* locus, was identified as a recurrent target of copy number gain and gene amplification. Furthermore, DNA sequencing of *ALK* revealed eight novel missense mutations in 13 out of 215 (6.1%) fresh tumours and 8 out of 24 (33%) neuroblastoma-derived cell lines. All but one mutation in the primary samples (12 out of 13) were found in stages 3–4 of the disease and were harboured in the kinase domain. The mutated kinases were autophosphorylated and displayed increased kinase activity compared with the wild-type kinase. They were able to transform NIH3T3 fibroblasts as shown by their colony formation ability in soft agar and their capacity to form tumours in nude mice. Furthermore, we demonstrate that downregulation of *ALK* through RNA interference suppresses proliferation of neuroblastoma cells harbouring mutated *ALK*. We anticipate that our findings will provide new insights into the pathogenesis of advanced neuroblastoma and that *ALK*-specific kinase inhibitors might improve its clinical outcome.

To identify oncogenic lesions in neuroblastoma, we performed a genome-wide analysis of primary tumour samples obtained from 215 neuroblastoma patients using high-density single-nucleotide polymorphism (SNP) arrays (Affymetrix GeneChip 250K *Nsp*I) (Supplementary Table 1). Twenty-four neuroblastoma-derived cell lines were also analysed (Supplementary Table 2). Interrogating over 250,000 SNP sites, this platform permits the identification of copy number changes at an average resolution of less than 12 kilobases (kb)[13,14].

Analysis of this large number of samples, consisting of varying disease stages, permitted us to obtain a comprehensive registry of genomic lesions in neuroblastoma (Supplementary Figs 1 and 2). A gain of chromosomes, often triploid or hyperploid (defined by mean copy number of >2.5), was a predominant feature of neuroblastoma genomes in the lower stages. Ploidy generally correlated with the clinical stage, where non-hyperploid cases were significantly associated with stage 4 disease ($P = 4.13 \times 10^{-5}$, trend test) (Supplementary Fig. 3 and Supplementary Table 3). 17q gains, frequently in multiple copies (3≤ copy number <5), were a hallmark of the neuroblastoma genome[4] and were found in most neuroblastoma cases. Copy number gains tended to spare chromosomes 3, 4, 10, 14 and 19 (Supplementary Figs 2 and 3). Notably, these chromosomes often had copy number losses including 1p (22.8%), 3p (8.8%), 4p (5.1%), 6q (7.0%), 10q (9.8%), 11q (19.5%), 14q (3.7%), 19p (7.4%) and 19q (5.1%), implicating the pathogenic role of 'relative' gene dosages.

After excluding known copy number variations, we identified a total of 28 loci undergoing high-grade amplifications (copy number ≥5) (Supplementary Table 4). These lesions fell into relatively small genomic segments, having a mean size of 361 kb, which accelerated the identification of gene targets in these regions (Supplementary Table 4 and Supplementary Fig. 4). The candidate gene targets included *TERT* (5p15.33), *HDAC3* (5q31.3), *IGF2* (11p15.1), *MYEOV* (11q13.3), *FGF7* (15q21.1) and *CDH13* (16q23.3). However, many of them were not recurrent but found only in a single case. Although the recurrent lesions were mostly explained by the amplification of *MYCN* at 2p24, as found in 50 out of 215 (23%) of the primary cases, we identified another peak of recurrent amplification at 2p23 (Fig. 1a), which consisted of amplicons in five primary cases and in one neuroblastoma-derived cell line, NB-1 (Supplementary Fig. 5). This peak was located at the centromeric margin of the common copy number gains in chromosome 2p, which was created by copy number gains in 109 samples mostly from non-hyperploid stage 4 cases. The minimum overlapping amplification was defined by the amplicons found in the NB-1 cell line (Supplementary Fig. 5) and contained a single gene, the anaplastic lymphoma kinase (*ALK*), which has previously been reported to be overexpressed in neuroblastoma cases[15]. Although five of the six samples showing *ALK* amplification also had *MYCN* amplification, one primary case (NT056) lacked a *MYCN* peak and the amplification was confined to the *ALK*-containing locus. In interphase fluorescent *in situ* hybridization (FISH) analysis of NB-1, *MYCN* and *ALK* loci were amplified in separate amplicons (Fig. 1b), indicating that the 2p23 amplicons containing *ALK* were unlikely to represent merely 'passenger' events of *MYCN* amplification but actively contributed to the pathogenesis of neuroblastoma.

Because an oncogene can be activated by gene amplification and/or mutation, to search for possible mutations we performed DNA heteroduplex formation analysis[16] and genomic DNA sequencing for the exons 20 to 28 of *ALK*, which encompass the juxtamembrane and kinase domains (Supplementary Table 5). In total, we identified eight nucleotide changes in 21 neuroblastoma samples, 13 out of 215

[1]Department of Pediatrics, [2]Cell Therapy and Transplantation Medicine, [3]Cancer Genomics Project, Graduate School of Medicine, The University of Tokyo, Tokyo 113-8655, Japan. [4]Division of Functional Genomics, Jichi Medical University, Toguchi 329-0498, Japan. [5]Division of Biochemistry, Chiba Cancer Center Research Institute, Chiba 260-8717, Japan. [6]Core Research for Evolutional Science and Technology, Japan Science and Technology Agency, Saitama, 332-0012, Japan. [7]Division of Hematology/Oncology, Saitama Children's Medical Center, Saitama 339-8551, Japan. [8]Gunma Children's Medical Center, Shibukawa 377-8577, Japan.
*These authors contributed equally to this work.